1Bd or pcD2E(−) were named B(+)1, 2, 3, 4, and 5 or B(−)1, 2, 3, 4, and 5, respectively. We confirmed the expression of the *ATDC* gene in these clones by RT-PCR (Fig. 2A). The *ATDC*-transcript was detected in clones S(+)1–5 and B(+)1–5, and it was not detected in clones S(−)1–5 or clones B(−)1–5 (Fig. 2A). ATDC protein was detected as a band having a molecular weight of 65 kDa in clones S(+)1–5 and B(+)1–5 and it was not detected in clones S(−)1–5 or B(−)1–5 (Fig. 2B).

Suppression of colony-forming efficiency by ATDC expression

Anchorage-independent growth *in vitro* is reported to correlate with the malignant phenotype *in vivo* [18]. The effect of *ATDC* expression on colony-forming efficiency in soft agar is shown in Table 1. Colony-forming efficiency in soft agar was significantly suppressed in all of clones S(+)1, 2, 3, 4 and 5 and B(+)1, 2, 3, 4 and 5 compared with the average value of clones S(−)1, 2, 3, 4 and 5 and that of clones B(−)1, 2, 3, 4 and 5, respectively (Table 1). Similarly, the average values of colony-forming efficiency of clones S(+)1, 2, 3, 4 and 5 and B(+)1, 2, 3, 4 and 5 were significantly lower than that of clones S(−)1, 2, 3, 4 and 5 and that of clones B(−)1, 2, 3, 4 and 5, respectively.

Effects of ATDC expression on cell proliferation

Effects of *ATDC* expression on cell proliferation were also examined. Cell proliferation rates of clones S(+)1, 2, 3, 4 and 5 and B(+)1, 2, 3, 4 and 5 tended to be lower than those of clones S(−)1, 2, 3, 4 and 5 and clones B(−)1, 2, 3, 4 and 5, respectively (Table 1, Figs. 3A and C). However, no significant difference was observed between the average value of cell proliferation rates of clones S(+)1–5 and that of clones S(−)1–5, and between that of clones B(+)1–5 and

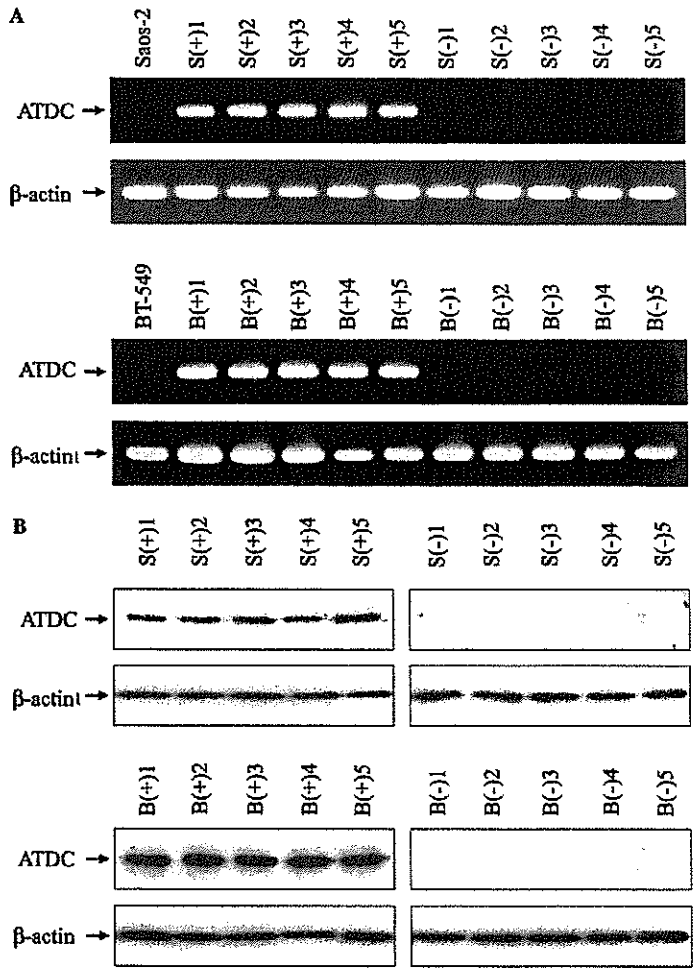

Fig. 2. RT-PCR assays and Western blot analysis of *ATDC* expression in Saos-2 and BT-549 cells transfected with the *ATDC* expression vector. (A) Total RNA was reverse transcribed and the products were amplified. Expected sizes of PCR products for *ATDC* and β-actin mRNA are 699 and 218 bp, respectively. (B) ATDC and β-actin proteins were detected by Western blot analysis using anti-ATDC antibody N-19 or anti-β-actin antibody AC-15. Details are the same as in Fig. 1B.

Table 1
Effects of *ATDC* expression on colony-forming efficiency in soft agar and cell proliferation rate

Cell	Colony-forming efficiency[a]	Cell proliferation rate[b]
Average of clones S(+)1–5	$4.90 \times 10^{4} \pm 5.04 \times 10^{4}$[c]	12.42 ± 2.97
Average of clones S(−)1–5	$8.84 \times 10^{2} \pm 3.69 \times 10^{2}$	14.94 ± 2.97
S(+)1	$1.17 \times 10^{4} \pm 7.64 \times 10^{5}$[c]	11.62 ± 1.12
S(+)2	$6.67 \times 10^{4} \pm 5.03 \times 10^{4}$[c]	16.09 ± 1.49
S(+)3	$1.67 \times 10^{4} \pm 1.16 \times 10^{4}$[c]	11.52 ± 0.94
S(+)4	$2.00 \times 10^{4} \pm 1.00 \times 10^{4}$[c]	7.74 ± 0.34
S(+)5	$1.30 \times 10^{3} \pm 9.85 \times 10^{4}$[c]	15.11 ± 0.78
S(−)1	$1.06 \times 10^{1} \pm 1.74 \times 10^{2}$	9.25 ± 0.64
S(−)2	$8.87 \times 10^{2} \pm 7.02 \times 10^{3}$	16.96 ± 1.06
S(−)3	$9.73 \times 10^{2} \pm 1.52 \times 10^{2}$	14.85 ± 2.98
S(−)4	$1.08 \times 10^{1} \pm 3.24 \times 10^{2}$	16.20 ± 0.98
S(−)5	$2.73 \times 10^{2} \pm 6.43 \times 10^{3}$	17.42 ± 1.43
Average of clones B(+)1–5	$3.80 \times 10^{5} \pm 1.46 \times 10^{5}$[d]	7.11 ± 3.80
Average of clones B(−)1–5	$6.81 \times 10^{3} \pm 3.64 \times 10^{3}$	8.49 ± 0.93
B(+)1	$3.67 \times 10^{5} \pm 1.53 \times 10^{5}$[d]	4.86 ± 0.37
B(+)2	$3.00 \times 10^{5} \pm 1.00 \times 10^{5}$[d]	3.20 ± 0.23
B(+)3	$6.33 \times 10^{5} \pm 3.06 \times 10^{5}$[d]	11.61 ± 0.67
B(+)4	$3.33 \times 10^{5} \pm 1.53 \times 10^{5}$[d]	11.82 ± 0.36
B(+)5	$2.67 \times 10^{5} \pm 1.53 \times 10^{5}$[d]	4.04 ± 0.26
B(−)1	$6.73 \times 10^{3} \pm 9.87 \times 10^{4}$	8.98 ± 0.40
B(−)2	$5.07 \times 10^{3} \pm 1.80 \times 10^{3}$	8.36 ± 0.42
B(−)3	$4.13 \times 10^{3} \pm 1.29 \times 10^{3}$	9.15 ± 0.26
B(−)4	$2.60 \times 10^{3} \pm 1.00 \times 10^{3}$	9.22 ± 0.31
B(−)5	$1.07 \times 10^{2} \pm 1.79 \times 10^{3}$	6.72 ± 0.54

[a] Cells were incubated for 56 days in a CO_2 incubator and colonies that consisted of more than 50 cells were counted. S(+)1, 2, 3, 4, and 5, and S(−)1, 2, 3, 4, and 5 are clones derived from the Saos-2 cells transfected with the *ATDC* expression vector pcD2E-1Bd and the control vector pcD2E, respectively. B(+)1, 2, 3, 4, and 5, and B(−)1, 2, 3, 4, and 5 are clones derived from the BT-549 cells transfected with pcD2E-1Bd and pcD2E, respectively. Means ± SD, $n = 3$ (S(+)1–5, S(−)1–5, B(+)1–5, and B(−)1–5) or $n = 5$ (averages of clones S(+)1–5, S(−)1–5, B(+)1–5, and B(−)1–5).

[b] Cell proliferation rate is expressed as the relative value, which is a value relative to the cell number at subculturing that is set to a value of 1, at 8 days for S(+)1–5 and S(−)1–5 or 4 days for B(+)1–5 and B(−)1–5 after subculturing. Means ± SD, $n = 5$.

[c] $P < 0.01$ compared with average of clones S(−)1–5.

[d] $P < 0.05$ compared with average of clones B(−)1–5.

that of clones B(−)1–5 (Table 1, Figs. 3B and D). No significant correlation was observed between cell proliferation rate and colony-forming efficiency in soft agar (Table 1).

Discussion

It has been reported that anchorage-independent growth correlates with the malignant phenotype *in vivo* [18]. In the present study, transfection of *ATDC* expression vector into the cells lacking *ATDC* expression suppressed colony-forming efficiency in soft agar, which suggests that no-expression/under-expression of *ATDC* is associated with a neoplastic phenotype.

Colony-forming efficiency in soft agar was suppressed by expression of *ATDC*, whereas cell proliferation was not affected by expression of *ATDC* (Table 1, Fig. 3). In a previous study, transfection of *RB* suppressed colony-forming efficiency in soft agar, but it did not affect the growth rate [18]. Similarly, transfection of wild-type p53 into neuroepithelioma A673 resulted in suppression of colony-forming efficiency in soft agar, but the growth rate was not affected by the transfection [19]. Suppression of colony-forming efficiency in soft agar and unaffected growth rate may be the phenotype associated with genes involved in carcinogenesis. The suppression of colony-forming efficiency in soft agar observed in the *ATDC*-transfectants is not due to the reduced growth rate because the *ATDC*-transfection did not affect the growth rate and there is no significant correlation between cell proliferation and colony-forming efficiency in soft agar (Table 1, Fig. 3). The suppression of colony-forming efficiency in soft agar by *ATDC*-transfection is smaller than that by the transfection of *RB* or *p53* [19,20], which indicates that the importance of *ATDC* in carcinogenesis might be less than that of *RB* or *p53*.

Underexpression of *ATDC* in breast cancer has been reported by Nacht et al. [14]. They examined *ATDC* expression using SAGE and DNA microarray analysis in 7 primary breast tumor tissues, 10 metastatic samples, and 4 normal tissues obtained immediately after surgical resection. *ATDC* was under-expressed with average 5.13-fold difference in primary tumors and with average 5.44-fold difference in metastatic tumors. Underexpression of *ATDC* in prostate cancer has been also reported [15]. Ernst et al. examined *ATDC* expression using DNA microarray analysis in 17 primary prostate cancer tissues and 9 normal adjacent tissues obtained immediately after surgical resection. *ATDC* was under-expressed with average 5.4-fold difference in prostate cancer tissues. They further confirmed underexpression of *ATDC* by real-time PCR assay using a part of the same samples. In the present study, we examined 6 breast cancer cell lines and found that one cell line did not express detectable *ATDC* mRNA. Nacht et al. reported that *ATDC* was more than 100-fold under-expressed in one metastatic breast cancer sample [14]. These results suggest that some of breast cancers express no *ATDC* mRNA or express *ATDC* mRNA at extremely low levels, which might have relevance to their malignant phenotype.

Brzosk et al. reported that *ATDC* was localized to cytoplasmic filaments [8]. Transformation affects the cytoskeletal organization, including actin and vimentin [21]. It has been reported that actin gene is a transcriptional target of p53, and that Ras induces actin rearrangement [22,23].

Multiple transcripts observed in Fig. 1A consisted chiefly of 3.0, 2.4, and 1.6 kbp mRNA. We previously reported the presence of at least eight sizes of mRNA (0.8, 1.6, 1.8, 2.4, 2.6, 3.0, 3.4, and 4.7 kbp) [10]. Because *ATDC* is present as a single copy gene [1], these multiple transcripts are due to alternative processing and/or multiple 5′ and 3′ ends. Tauchi et al. cloned 2.4 kbp transcript of *ATDC* using HeLa cell cDNA library and reported that the 2.4 kbp transcript is untranslated because it has a stop

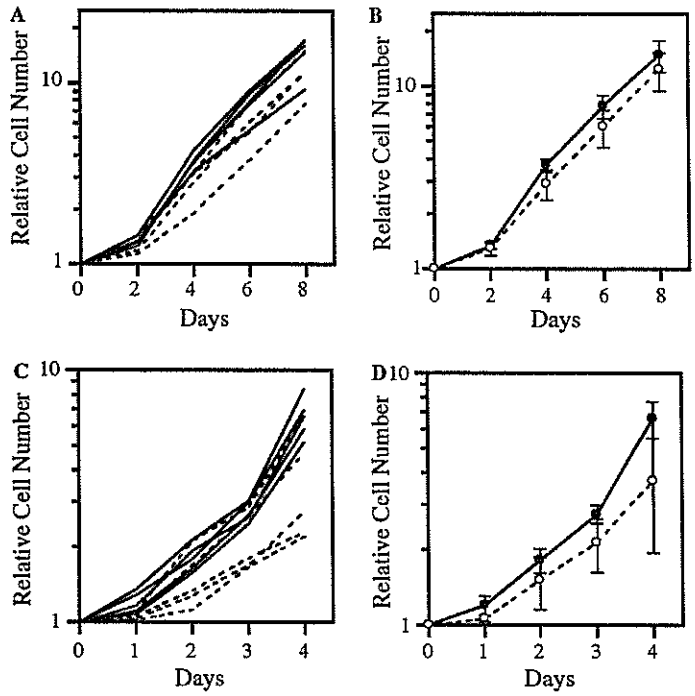

Fig. 3. Effect of *ATDC* expression on cell proliferation. Cell numbers are expressed as values relative to the number at subculturing, which is set to a value of 1. (A) Cell proliferation curves for clones S(+)1–5 and S(−)1–5. Solid lines show cell proliferation curves for clones S(−)1–5 and dotted lines show those for clones S(+)1–5, respectively. (B) Average cell proliferation curves for clones S(−)1–5 (means ± SD of the values of clones S(−)1–5) (●) and for clones S(+)1–5 (means ± SD of the values of clones S(+)1–5) (○). (C) Cell proliferation curves of clones B(+)1–5 and B(−)1–5. Solid lines show cell proliferation curves for clones B(−)1–5 and dotted lines show those for clones B(+)1–5, respectively. (D) Average cell proliferation curves for clones B(−)1–5 (means ± SD of the values of clones B(−)1–5) (●) and for clones B(+)1–5 (means ± SD of the values of clones B(+)1–5) (○).

codon located 33 bp in front of the first methionine [24]. On the other hand, a variant transcript of *ATDC* (tripartite motif-containing 29, TRIM29) has been reported, which has an additional exon at the end of the coding region of the 3.0 kbp *ATDC* cDNA (GenBank, NM_058193). The full-length nature of *ATDC*/TRIM29 has not been described yet, and it is still unknown whether the 65 kDa protein is only the functional ATDC protein.

ATDC may be related to both carcinogenesis and radiation sensitivity through its cytoskeletal organization and/or its role in regulation of PKC. However, detailed biological functions of ATDC are not well known, and further examination is required for their elucidation.

References

[1] L.N. Kapp, R.B. Painter, L.C. Yu, N. van Loon 3rd, C.W. Richard, M.R. James, D.R. Cox, J.P. Murnane, Cloning of a candidate gene for ataxia-telangiectasia group D, Am. J. Hum. Genet. 51 (1992) 45–54.

[2] J.P. Murnane, L.N. Kapp, A critical look at the association of human genetic syndromes with sensitivity to ionizing radiation, Semin. Cancer Biol. 4 (1993) 93–104.

[3] L.N. Kapp, R.B. Painter, Stable radioresistance in ataxia-telangiectasia cells containing DNA from normal human cells, Int. J. Radiat. Biol. 56 (1989) 667–675.

[4] E.A. Leonhardt, L.N. Kapp, B.R. Young, J.P. Murnane, Nucleotide sequence analysis of a candidate gene for ataxia-telangiectasia group D (ATDC), Genomics 19 (1994) 130–136.

[5] B.A. Reddy, L.D. Etkin, P.S. Freemont, A novel zinc finger coiled-coil domain in a family of nuclear proteins, Trends Biochem. Sci. 17 (1992) 344–345.

[6] K.L. Borden, RING fingers and B-boxes: zinc-binding protein-protein interaction domains, Biochem. Cell Biol. 76 (1998) 351–358.

[7] A. Reymond, G. Meroni, A. Fantozzi, G. Merla, S. Cairo, L. Luzi, D. Riganelli, E. Zanaria, S. Messali, S. Cainarca, A. Guffanti, S. Minucci, P.G. Pelicci, A. Ballabio, The tripartite motif family identifies cell compartments, EMBO J. 20 (2001) 2140–2151.

[8] P.M. Brzoska, H. Chen, Y. Zhu, N.A. Levin, M.H. Disatnik, D. Mochly-Rosen, J.P. Murnane, M.F. Christman, The product of the ataxia-telangiectasia group D complementing gene, ATDC, interacts with a protein kinase C substrate and inhibitor, Proc. Natl. Acad. Sci. USA 92 (1995) 7824–7828.

[9] K.R. Laderoute, A.M. Knapp, C.J. Green, R.M. Sutherland, L.N. Kapp, Expression of the ATDC (ataxia telangiectasia group D-complementing) gene in A431 human squamous carcinoma cells, Int. J. Cancer 66 (1996) 772–778.

[10] Y. Hosoi, L.N. Kapp, Expression of a candidate ataxia-telangiectasia group D gene in cultured fibroblast cell lines and human tissues, Int. J. Radiat. Biol. 66 (1994) S71–S76.

[11] D.P. Lane, L.V. Crawford, T antigen is bound to a host protein in SV40-transformed cells, Nature 278 (1979) 261–263.

[12] J.A. DeCaprio, J.W. Ludlow, J. Figge, J.Y. Shew, C.M. Huang, W.H. Lee, E. Marsilio, E. Paucha, D.M. Livingston, SV40 large tumor antigen forms a specific complex with the product of the retinoblastoma susceptibility gene, Cell 54 (1988) 275–283.

[13] J. Koreth, P.B. Bethwaite, J.O. McGee, Mutation at chromosome 11q23 in human non-familial breast cancer: a microdissection microsatellite analysis, J. Pathol. 176 (1995) 11–18.
[14] M. Nacht, A.T. Ferguson, W. Zhang, J.M. Petroziello, B.P. Cook, Y.H. Gao, S. Maguire, D. Riley, G. Coppola, G.M. Landes, S.L. Madden, S. Sukumar, Combining serial analysis of gene expression and array technologies to identify genes differentially expressed in breast cancer, Cancer Res. 59 (1999) 5464–5470.
[15] T. Ernst, M. Hergenhahn, M. Kenzelmann, C.D. Cohen, M. Bonrouhi, A. Weninger, R. Klaren, E.F. Grone, M. Wiesel, C. Gudemann, J. Kuster, W. Schott, G. Staehler, M. Kretzler, M. Hollstein, H.J. Grone, Decrease and gain of gene expression are equally discriminatory markers for prostate carcinoma: a gene expression analysis on total and microdissected prostate tissue, Am. J. Pathol. 160 (2002) 2169–2180.
[16] J.P. Murnane, Inducible gene expression by DNA rearrangements in human cells, Mol. Cell. Biol. 6 (1986) 549–558.
[17] K. Takayama, E.P. Salazar, A. Lehmann, M. Stefanini, L.H. Thompson, C.A. Weber, Defects in the DNA repair and transcription gene ERCC2 in the cancer-prone disorder xeroderma pigmentosum group D, Cancer Res. 55 (1995) 5656–5663.
[18] R. Takahashi, T. Hashimoto, H.J. Xu, S.X. Hu, T. Matsui, T. Miki, H. Bigo-Marshall, S.A. Aaronson, W.F. Benedict, The retinoblastoma gene functions as a growth and tumor suppressor in human bladder carcinoma cells, Proc. Natl. Acad. Sci. USA 88 (1991) 5257–5261.
[19] Y.M. Chen, P.L. Chen, N. Arnaiz, D. Goodrich, W.H. Lee, Expression of wild-type p53 in human A673 cells suppresses tumorigenicity but not growth rate, Oncogene 6 (1991) 1799–1805.
[20] W.B. Isaacs, B.S. Carter, C.M. Ewing, Wild-type p53 suppresses growth of human prostate cancer cells containing mutant p53 alleles, Cancer Res. 51 (1991) 4716–4720.
[21] E.J. Hansell, S.M. Frisch, P. Tremble, J.P. Murnane, Z. Werb, Simian virus 40 transformation alters the actin cytoskeleton, expression of matrix metalloproteinases and inhibitors of metalloproteinases, and invasive behavior of normal and ataxia-telangiectasia human skin fibroblasts, Biochem. Cell Biol. 73 (1995) 373–389.
[22] K.A. Comer, P.A. Dennis, L. Armstrong, J.J. Catino, M.B. Kastan, C.C. Kumar, Human smooth muscle alpha-actin gene is a transcriptional target of the p53 tumor suppressor protein, Oncogene 16 (1998) 1299–1308.
[23] P. Rodriguez-Viciana, P.H. Warne, A. Khwaja, B.M. Marte, D. Pappin, P. Das, M.D. Waterfield, A. Ridley, J. Downward, Role of phosphoinositide 3-OH kinase in cell transformation and control of the actin cytoskeleton by Ras, Cell 89 (1997) 457–467.
[24] H. Tauchi, C. Green, M. Knapp, K. Laderoute, L. Kapp, Altered splicing of the ATDC message in ataxia telangiectasia group D cells results in the absence of a functional protein, Mutagenesis 15 (2000) 105–108.

Heterogeneous expression of DNA-dependent protein kinase in esophageal cancer and normal epithelium

NORIO TONOTSUKA[1,2], YOSHIO HOSOI[4], SHUKICHI MIYAZAKI[2], GO MIYATA[2], KO SUGAWARA[2], TAKAHIRO MORI[3], NORIAKI OUCHI[3], SUSUMU SATOMI[2], YOSHIHISA MATSUMOTO[4], KEIICHI NAKAGAWA[5], KIYOSHI MIYAGAWA[4] and TETSUYA ONO[1]

[1]Department of Radiation Research, [2]Division of Advanced Surgical Science and Technology and [3]Division of Surgical Oncology, Faculty of Medicine, Tohoku University, Sendai 980-8575; Departments of [4]Radiation Research and [5]Radiology, Faculty of Medicine, University of Tokyo, Tokyo 113-0033, Japan

Received February 10, 2006; Accepted April 13, 2006

Abstract. Esophageal cancer tissues and adjacent normal mucosae in 13 patients with primary esophageal cancer were examined for quantitative differences in DNA-dependent protein kinase (DNA-PK) activity and for expressions of Ku70, Ku80 and DNA-PKcs proteins by Western blotting and immunohistochemistry. The tumor tissues showed higher DNA-PK activity than the normal mucosae. Protein levels of Ku70, Ku80 and DNA-PKcs correlated with DNA-PK activities in the tumor tissues. Immunohistochemical analysis revealed that Ku70, Ku80 and DNA-PKcs located predominantly in the nuclei in both the tumor tissues and normal mucosae. In the normal epithelium, Ku70, Ku80 and DNA-PKcs were expressed only in the nuclei of the basal cell layers and not in those of the lumenal cell layers. In the tumor tissues, the expressions of DNA-PK proteins showed intratumoral heterogeneity. The different portions in the same tumor showed different expression levels of DNA-PK proteins, and even each tumor cell showed different expression levels. These results suggest that cell differentiation and tumor progression affect cellular DNA-PK protein levels and its activity. Furthermore, the intratumoral heterogeneity of DNA-PK protein expression in esophageal cancer cells/tissues also suggests the difficulty in prediction of radio- or chemo-sensitivity of the tumor through estimation of DNA-PK activity/protein levels in tumor specimens.

Introduction

DNA-dependent protein kinase (DNA-PK) is a nuclear protein with serine/threonine kinase activity and it composed of the catalytic subunit of DNA-PK (DNA-PKcs) and a heterodimer of Ku70 and Ku80 (1). DNA-PK plays a crucial role in the repair of DNA double-strand breaks (DSBs) induced by ionizing radiation and chemotherapeutic agents (1). Cells lacking DNA-PK activity because of defects in the DNA-PK components show hypersensitivity to ionizing radiation and chemotherapeutic agents (2-6).

There have been many reports on the examination whether DNA-PK activity correlates with radiation sensitivity and whether it can be a parameter indicating the sensitivity to radiotherapy and/or chemotherapy. Suppression of DNA-PK activity by a phosphatidylinositol 3-kinase inhibitor wortmannin, antisense Ku70/DNA-PKcs, or small inhibitory RNA for DNA-PKcs sensitized cells to ionizing radiation (7-10). Polischouk *et al* reported that levels of DNA-PK activity associate with the proficiency in rejoining of DNA double-strand breaks (11). These results indicate that levels of DNA-PK activity correlates with cellular sensitivity to ionizing radiation in the cells under the same genetic background. Relationship between radiation sensitivity and DNA-PK activity/protein levels under different genetic backgrounds has been investigated in cultured cell lines or tissue specimens obtained from patients with cancer (11-20). The results reported were contradictory and it is still unclear whether DNA-PK can be a parameter indicating radiation sensitivity under different genetic backgrounds.

To predict curability of the tumor after radiotherapy or chemotherapy, the sensitivities in both tumor tissue and adjacent normal tissue should be assessed. We previously examined the DNA-PK activities in tumor tissues and adjacent normal tissues in patient with colorectal cancer and found that the tumor tissues showed higher DNA-PK activity than the adjacent normal tissues in 11 out of 12 patients, which suggests poor curability of the tumors after radiation therapy alone under the condition that the DNA-PK activity correlates with radiation sensitivity (21). In the present study, we examined DNA-PK activities and protein levels of the tumor tissues and the adjacent normal mucosae in patients with esophageal cancer by the standard kinase activity assay, Western blotting and immunohistochemistry. The results revealed that DNA-PK activity was higher in esophageal

Correspondence to: Dr Yoshio Hosoi, Department of Radiation Research, Faculty of Medicine, University of Tokyo, 7-3-1 Hongo, Bunkyoku, Tokyo 113-0033, Japan
E-mail: hosoi@m.u-tokyo.ac.jp

Key words: DNA-dependent protein kinase, esophageal cancer, Ku70, Ku80, DNA-PKcs

Table I. Characteristics of the patients.

Patient No.	Sex	Position[a]	Histology[b]	Differentiation	pTNM[c]
1	M	Lt	SCC	Poorly differentiated	III
2	F	Mt	SCC	Well differentiated	III
3	F	Mt	SCC	Poorly differentiated	I
4	M	Ce	SCC	Poorly differentiated	III
5	M	Mt	SCC	Moderately differentiated	I
6	M	Mt	SCC	Well differentiated	III
7	F	Lt	Undifferentiated	Undifferentiated	IIB
8	F	Lt	SCC	Moderately differentiated	IIB
9	M	Mt	Basaloid	-	III
10	F	Mt	SCC	Well differentiated	I
11	M	Lt	SCC	Poorly differentiated	IIA
12	M	Ae	SCC	Poorly differentiated	IIB
13	M	Mt	SCC	Poorly differentiated	I

[a]Ce, cervical esophagus; Mt, middle thoracic esophagus; Lt, lower thoracic esophagus; Ae, abdominal esophagus. [b]SCC, squamous cell carcinoma; undiffrentiated, Undifferentiated carcinoma (small cell type); basaloid, basaloidcarcinoma. [c]pTNM, pathological stage grouping according to TNM classification.

cancer tissues than in the normal mucosae and that the levels of DNA-PK proteins correlated with the DNA-PK activity. Expressions of DNA-PK proteins in tumor tissues were found to be heterogeneous, which suggests the difficulty in prediction of radio- or chemo-sensitivity of the tumors thorough the examination of DNA-PK activity/protein levels in tumor specimens of esophageal cancer.

Materials and methods

Tissue specimens. All esophageal tumors and adjacent normal tissues were obtained at the time of surgery at Tohoku University Hospital from 1999 to 2000. Informed consent was received from all patients. The patients received neither radiotherapy nor chemotherapy before surgery. Characteristics of the patients are shown in Table I.

Cells. LM217 is an SV40 transformed human fibroblast cell line derived from HS27 (22). LM217 was used as control in measurement of DNA-PK activity and Western blotting.

Whole-cell and tissue extracts. Whole-cell extracts and tissue extracts were prepared by a modification of the methods of Finnie *et al* and Dignam *et al* (23,24). The samples were washed twice with Tris-buffered saline [2 mM Tris (pH 7.2), 150 mM NaCl], homogenized using a hand-operated homogenizer (Eppendorf, Hamburg, Germany), then suspended in 100 μl of a low-salt buffer [10 mM HEPES (pH 7.2), 25 mM KCl, 10 mM NaCl, 1.1 mM $MgCl_2$, 1 mM EDTA, 1 mM EGTA, 1 mM PMSF, 1 mM DTT, 1 μg/ml pepstatin, 1 μg/ml leupeptin, 1 μg/ml antipain], and then frozen in liquid nitrogen and thawed at 30°C three times. After a 60-min incubation at 4°C, the suspension was adjusted to 0.4 M KCl by adding 3.5 M KCl, incubated for 30 min at 4°C, and centrifuged for 10 min at 15,000 rpm. The supernatant was designated as the whole-cell extract (25). Protein concentrations were determined with the Bio-Rad protein assay (Bio-Rad, Hercules, CA).

DNA-PK activity. DNA-PK activity was assayed as previously described, with a synthetic peptide (EPPLSQEAFAD LWKK) (7). The whole-cell or tissue extracts were incubated in 20 μl of kinase buffer [20 mM HEPES-NaOH (pH 7.2), 100 mM KCl, 5 mM $MgCl_2$, 1 mM DTT, 0.5 mM NaF, 0.5 mM ß-glycerophosphate, 0.2 mM ATP, 10 μCi/ml [γ-^{32}P]ATP in the presence of 0.01 mg/ml sonicated salmon sperm DNA and 0.5 mg/ml substrate peptide] at 37°C for 15 min. The final protein concentration in the reaction mixture was 37.5 μg/ml. The reactions were stopped by the addition of 20 μl of 30% acetic acid and the mixtures were spotted onto P81 paper disks (Whatman International Ltd., Maidstone, UK). The disks were washed 4 times in 15% acetic acid. Radioactivity in the paper disks was measured in a liquid scintillation counter.

Western blotting. Whole cell extracts or tissue extracts were lysed in the electrophoresis sample buffer [62.5 mM Tris (pH 6.8), 2% SDS, 5% glycerol, 0.003% bromophenol blue, 1% ß-mercaptoethanol] and boiled for 5 min. The lysate was resolved by electrophoresis using a gradient gel (Daiichi Pure Chemicals Co., Ltd., Tokyo, Japan), and was electrophoretically transferred to polyvinylidene difluoride membranes (Bio-Rad). The membranes were then proved with anti-Ku70 antibody, anti-Ku80 antibody, anti-DNA-PKcs antibody Ab-4 (Cocktail) (NeoMarkers, Fremont, CA) or Anti-GAPDH antibody (Trevigen, Inc., Gaithersburg, MD). The anti-Ku70 and anti-Ku80 antibodies used were raised in our laboratory as previously reported (19). The antigen-antibody complexes were detected by the ECL Plus™ Western blotting detection reagents (Amersham Pharmacia Biotech Inc., Piscataway, NJ), with horseradish peroxidase-conjugated antibodies. The images were analyzed with the Scion Image Beta 4.02 Win software (Scion Corporation, Frederick, MD) to quantify the densities of bands corresponding to Ku70, Ku80, DNA-PKcs and GAPDH.

Immunohistochemistry for DNA-PK proteins. Formalin-fixed and paraffin-embedded tissue specimens were deparaffinized,

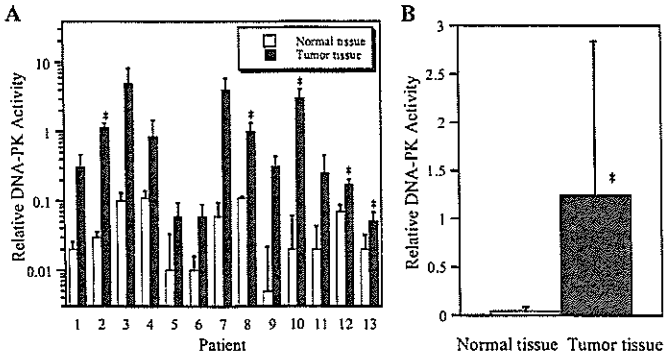

Figure 1. DNA-PK activities of tumor tissues and adjacent normal mucosae in 13 patients with esophageal cancer. DNA-PK activities are expressed as values relative to that of LM217, which is set to a value of 1. (A) Mean ± SD of DNA-PK activities of three different specimens of tumor tissues and normal tissues in each patient, *P<0.05. (B) Average values of DNA-PK activities of tumor tissues and normal tissues in 13 patients. Mean ± SD, *P<0.05.

cut to 2-μ sections, and stained by the labeled streptavidin biotin (LSAB) technique. Briefly, the sections were incubated with 3% hydrogen peroxide in methanol, and then incubated with 1% bovine serum for 30 min for blocking. The sections were incubated with primary antibody overnight at room temperature, and incubated with biotinylated secondary antibody (Nichirei Biosciences Inc., Tokyo, Japan) for 30 min at room temperature. Then, streptavidin/biotin complex was applied for 30 min (Nichirei Biosciences Inc.), followed by a 30 min incubation in 3,3'-diaminobnzidine substrate, yielding a brown reaction product. Sections were counterstained with hematoxylin and mounted under a coverslip.

Evaluation. The intensity of staining in immunohistochemistry was evaluated by the expression score reported by Rigas *et al* (26). The intensity of staining was rated according to the following scale: 2 = intense brown staining, 1 = light brown staining, 0 = no staining. In each sample, the percentage of cells expressing each protein was determined. To obtain a numerical assessment of the expression of each protein, we calculated the multiple of the intensity of staining by the percentage of cells expressing a protein for each sample. In tumor tissues, we assessed the expression score at the growing edge of the carcinoma, which is defined as the invasive tip, because tumor growth largely depends on the proliferative kinetics at the invasive tip (27). In normal tissues, the expression score was assessed at the normal mucosae. Each expression score was expressed as mean ± SD of three scores evaluated at the three different fields in the invasive tip or in normal mucosae respectively with original magnification of x400.

Statistics. Homogeneity of variance was tested by the F-test. When variance was homogeneous, Student's t-test was used. When variance was heterogeneous, Welch's test was used. For analysis of correlation coefficient, the distributions of variables were tested first. When variables were normally distributed, Peason's correlation coefficient test was used. When variables were not normally distributed, Spearman's rank correlation coefficient test was used. Differences were considered to be statistically significant at P<0.05.

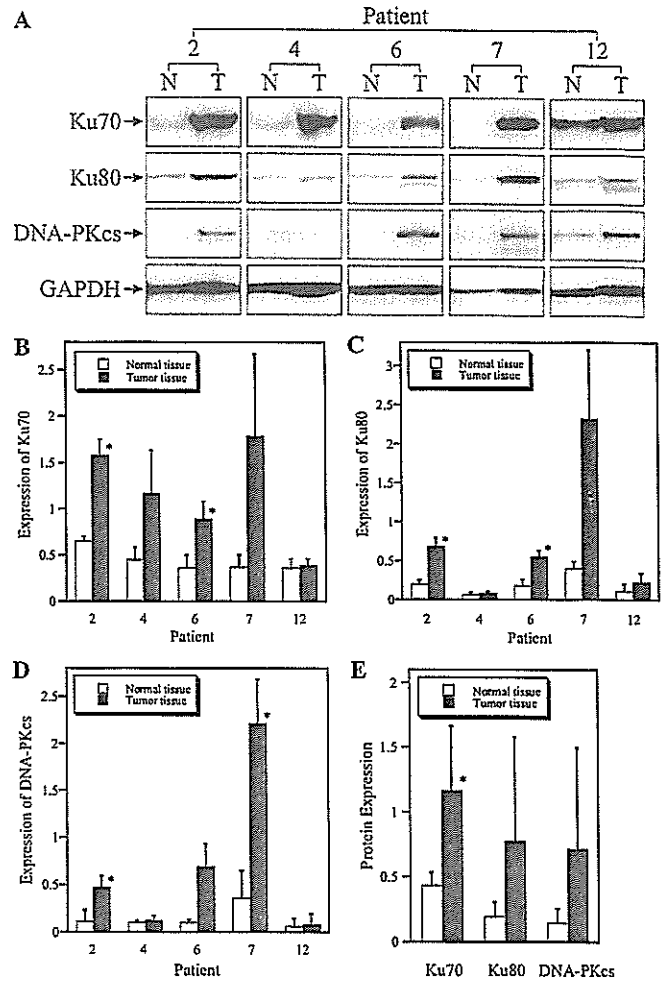

Figure 2. Expression of DNA-PK proteins in normal mucosae and tumor tissues. (A) Western blot analysis for Ku70, Ku80, DNA-PKcs and GAPDH in the extracts prepared from tumor tissues (T) and normal mucosae (N) obtained from patients No. 2, 4, 6, 7 and 12. (B-D) Relative protein levels of Ku70, Ku80 and DNA-PKcs in the 5 patients. Histograms represent the scanning densitometric analysis of Western blots. Each value is normalized for GAPDH and expressed as a value relative to that of LM217, which is set to a value of 1. Mean ± SD of the data from three different tissue extracts used in the measurement of DNA-PK activity. (E) Average values of Ku70, Ku80 and DNA-PKcs protein levels of tumor tissues and normal tissues in the 5 patients. Mean ± SD, *P<0.05.

Results

DNA-PK activity of tumor tissues and normal mucosae. We examined DNA-PK activities of tumor tissues and adjacent normal mucosae in 13 patients with esophageal cancer. In 5 patients, DNA-PK activity was significantly higher in the tumor tissue compared with the normal mucosa (Fig. 1A). Average value of the DNA-PK activities of the tumor tissues in the 13 patients was significantly higher than that of the normal mucosae (Fig. 1B).

Expression of DNA-PK proteins in tumor tissues and normal mucosae. Next, we examined DNA-PK protein levels by Western blotting in order to investigate whether the variety of DNA-PK activities observed in tumor tissues and normal mucosae depended on the DNA-PK protein levels. For the Western blotting, we used the same tissue extracts as used in the assessments of DNA-PK activity. Western blotting was

conducted using the tissue extracts from the 5 patients whose had enough tissue extracts for the Western blot analysis (Fig. 2A). In 2 out of the 5 patients, levels of Ku70, Ku80 and DNA-PKcs proteins were significantly higher in the tumor tissue compared with the normal mucosae (Fig. 2B-D). Average value of Ku70 protein levels in the 5 patients was significantly higher in the tumor tissue (Fig. 2E). Significant correlation was observed between DNA-PK activity and protein levels of Ku70, Ku80 and DNA-PKcs in tumor tissues of the 5 patients (Table IIB). Ku70 and Ku80 protein levels correlated with DNA-PKcs protein level in the tumor tissues (Table IIB). Ku70 protein level correlated with Ku80 protein level in the normal tissues (Table IIA).

Immunohistochemical analysis in normal mucosae. Esophageal epithelium consists of non-keratinized stratified squamous cells as shown in Fig. 3A. Stainings for Ku70, Ku80 and DNA-PKcs were predominantly nuclear and they showed a similar pattern (Fig. 3B-E). In the epithelium, Ku70, Ku80 and DNA-PKcs were expressed exclusively in the nuclei of the basal cell layers and not in those of the lumenal cell layers (Fig. 3B-D). The DNA-PK proteins were expressed in almost all the nuclei in the middle-basal cell layers of the epithelium, whereas they were not expressed in some nuclei in the most basal cell layers (Fig. 3B-D). In lamina propria and muscularis mucosa, the DNA-PK proteins were expressed in about half of the nuclei (Fig. 3B-D).

Immunohistochemical analysis in tumor tissues. In tumor tissues, stainings for Ku70, Ku80 and DNA-PKcs were also predominantly nuclear and they showed a similar pattern in each tumor (Figs. 4 and 5). The intensity of staining was heterogeneous in the tumor tissues (Figs. 4B-D and 5B-D). The different portions in the same tumor showed different expression levels of DNA-PK proteins, and even each tumor cell showed different expression levels (Figs. 4F-H and 5F-H). These heterogeneic staining patterns of the DNA-PK proteins could be observed in all the tumors examined.

A semi-quantitative assessment of DNA-PK proteins. To assess the expression of DNA-PK proteins semi-qantitatively in immunohistochemical examination, the intensity of staining was evaluated by the expression score described in Materials and methods. The expression score was significantly higher in the tumor tissue than in the normal mucosa in 7 patients for Ku70, 4 patients for Ku80 and 6 patients for DNA-PKcs (Fig. 6A-C). In 2 patients, the expression score for DNA-PKcs was lower in the tumor tissue than in the normal mucosa (Fig. 6C). The average values of expression scores for Ku70 and Ku80 in 13 patients were significantly higher in the tumor tissue than in the normal mucosa (Fig. 6D).

Table II. Correlation coefficient.

A, Correlation coefficients in normal tissues

	Ku70		Ku80		DNA-PKcs	
	P	CC	P	CC	P	CC
DNA-PK activity	0.323	-0.491	0.258	-0.550	0.975	0.975
Ku70	-	-	**0.0401**	0.816	0.725	0.157
Ku80	**0.041**	0.816	-	-	0.544	0.271
DNA-PKcs	0.725	0.157	0.544	0.271	-	-

B, Correlation coefficients in tumor tissues

	Ku70		Ku80		DNA-PKcs	
	P	CC	P	CC	P	CC
DNA-PK activity	**0.0476**	0.832	**0.00580**	0.937	**0.0100**	0.917
Ku70	-	-	0.101	0.728	**0.000285**	0.986
Ku80	0.101	0.728	-	-	**0.000284**	0.986
DNA-PKcs	**0.000285**	0.986	**0.000284**	0.986	-	-

CC, correlation coefficient. Bold values indicating $P<0.05$.

Discussion

Prediction of radio- and chemo-sensitivity of normal and tumor tissues before the treatment will provide crucial information to find the best treatment method for each patient with cancer. In most of the cells, cell survival after X-irradiation depends on the yield of DNA DSBs and the repair of them. Non-homologous end-joining (NHEJ) and homologous recombination (HR) are the two major repair mechanisms for DSBs, and NHEJ plays the most important role in mammalian cells (28). Radiation sensitivity can be possibly predicted through the quantitative evaluation of DNA-PK as a key enzyme for NHEJ because DNA-PK activity has relevance to cellular sensitivity to ionizing radiation and DNA-PK protein levels correlate with DNA-PK activity (7-11). In the present study, the immuno-histochemical analysis revealed the intratumoral heterogeneity of DNA-PK protein expression (Figs. 4 and 5). The different portions in the same tumor showed different expression levels of DNA-PK proteins, and even each tumor cell showed different expression levels (Figs. 4 and 5). This heterogeneous expression of DNA-PK proteins in esophageal cancer tissues suggests the difficulty in prediction of curability of the tumors after radiotherapy or chemotherapy through evaluation of DNA-PK protein levels in the tumor specimens because the curability will reflect the DNA-PK protein levels in the cells that express DNA-PK most abundantly in the tumor under the condition that radiation sensitivity correlates with DNA-PK activity.

In the present study, DNA-PK activity correlated with protein levels of Ku70, Ku80 and DNA-PKcs, and protein levels of Ku70 and Ku80 correlated with the levels of DNA-PKcs in tumor tissues (Table II). These results correspond with previous reports (16,18,20,21). Promoter regions of *Ku70*, *Ku80* and *DNA-PKcs* contain consensus Sp1 recognition elements and therefore these genes are supposed to be regulated by the same transcriptional factor, Sp1 (21,29,30).

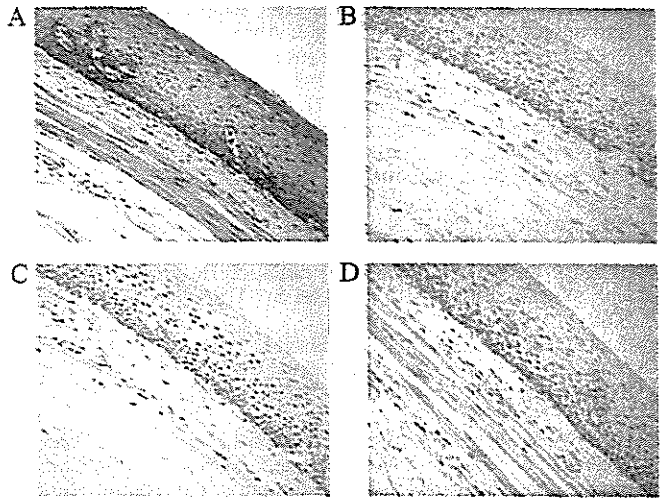

Figure 3. The expression of DNA-PK proteins in esophageal mucosae from patient No. 7. (A) Staining with hematoxylin and eosin. (B) Immunostaining for Ku70. (C) Immunostaining for Ku80. (D) Immunostaining for DNA-PKcs. Original magnification x100.

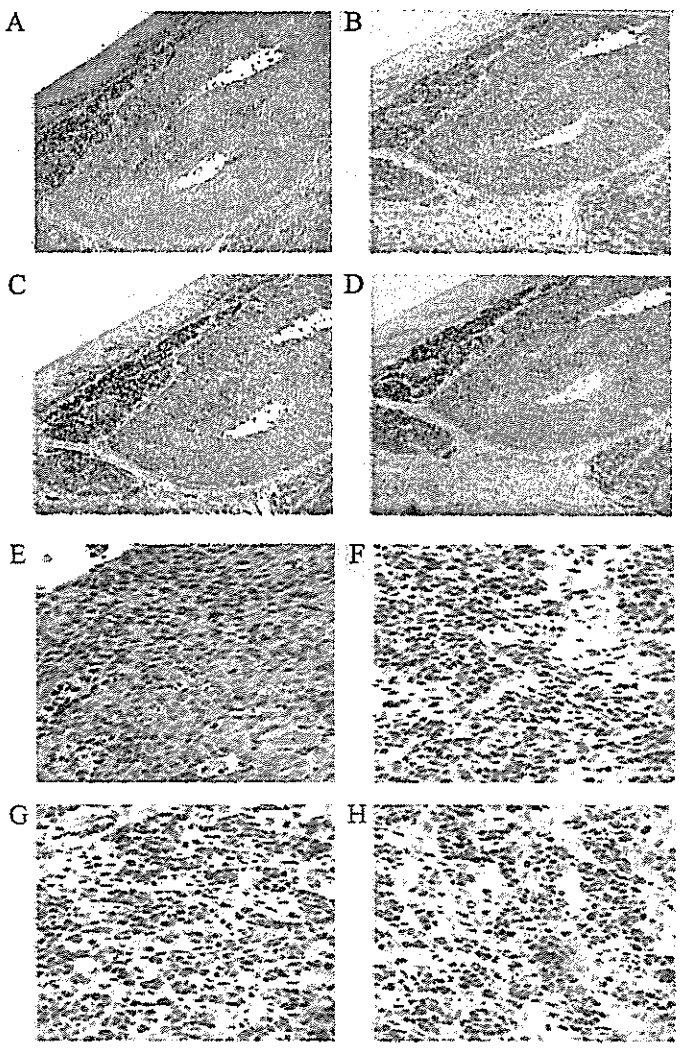

Figure 4. The expression of DNA-PK proteins in esophageal cancer tissues from patient No. 7. (A and E) Staining with hematoxylin and eosin. (B and F) Immunostaining for Ku70. (C and G) Immunostaining for Ku80. (D and H) Immunostaining for DNA-PKcs. Original magnification x16 (A-D) and x400 (E-H).

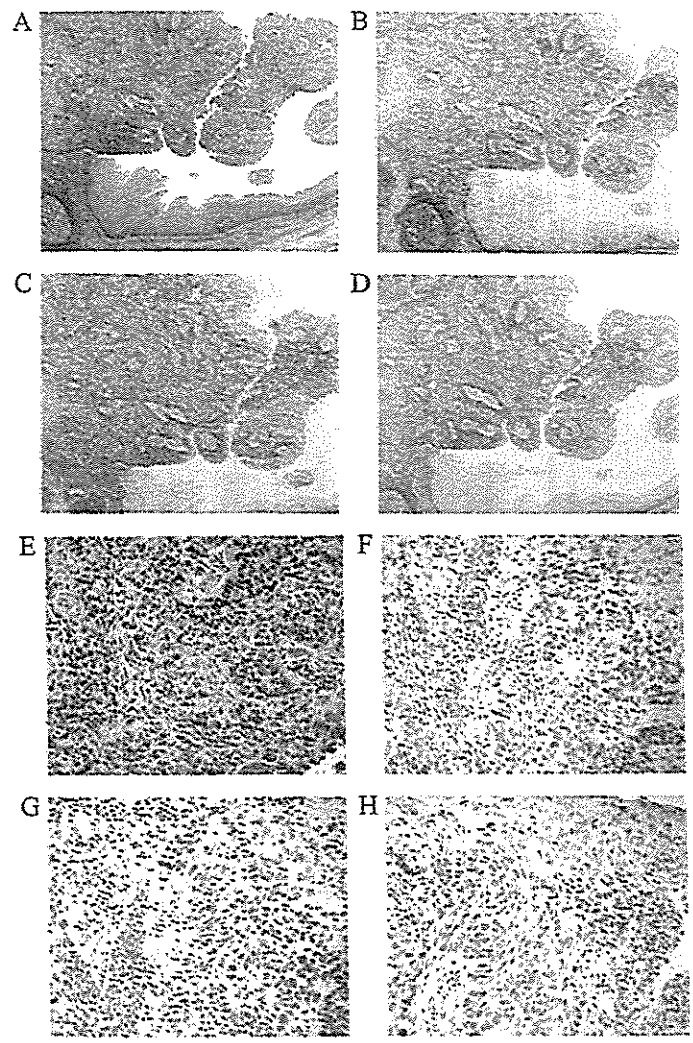

Figure 5. The expression of DNA-PK proteins in esophageal cancer tissues from patient No. 13. (A and E) Staining with hematoxylin and eosin. (B and F) Immunostaining for Ku70. (C and G) Immunostaining for Ku80. (D and H) Immunostaining for DNA-PKcs. Original magnification x16 (A-D) and x400 (E-H).

Sp1 biding sites are located in the promoter regions of a number of growth-regulated genes including insulin-like growth factor-binding protein 2 and vascular/endothelial growth factor (31,32). Suppression of Sp1 by dominant negative Sp1 and Sp1-site-decoy oligonucleotides induces cell growth arrest (32,33). These results suggest involvement of Sp1 in growth-regulation. In the present study, DNA-PK proteins were highly expressed in the nuclei of the basal cell layers of the normal epithelium and were not expressed in luminal cell layers (Fig. 3), which may reflect the growth of the stem cells located in the basal cell layers and the growth arrest of the differentiated cells in the luminal cell layers.

In the present study, the different portions in the same tumor showed different expression levels of DNA-PK proteins, and even each tumor cell showed different expression levels (Figs. 4 and 5). In esophageal cancer, intratumoral heterogeneity has been reported in expressions of many proteins includeing transcription factor Ets-1, cyclin B1, cyclin D1, retinoblastoma protein, cyclooxygenase-2, GAGE, NY-ESO-1, MAGE-A, SSX, E-cadherin and α-catein (34-40).

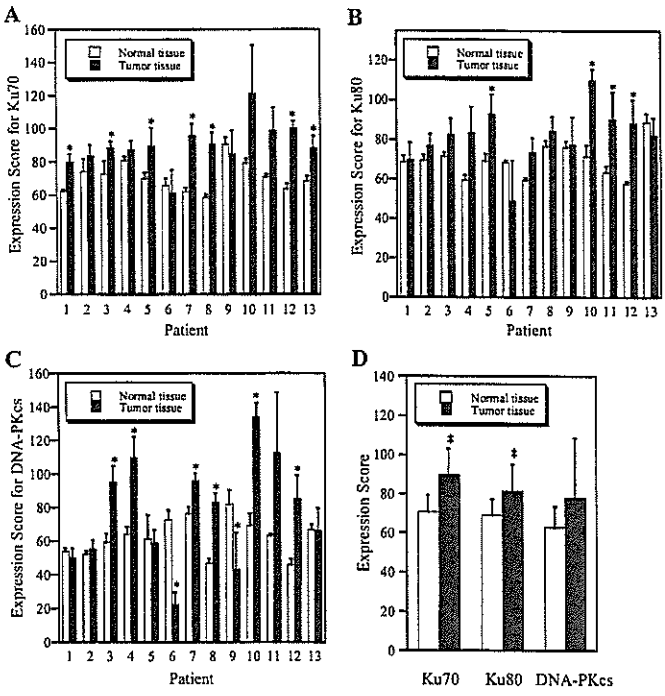

Figure 6. The expression of DNA-PK proteins in normal mucosae and tumor tissues estimated by the expression score. The expression score is the product of the intensity of expression multiplied by the percentage of cell expressing a given protein, and it assesses numerically the expression of each protein. Details are described in Materials and methods. (A and C) Expression scores for Ku70, Ku80 and DNA-PKcs in patients No. 1-13, respectively. Mean ± SD of three expression scores. (D) Average values of the expression scores in the 13 patients. Mean ± SD, *P<0.05.

It has been reported that esophageal cancer is genetically heterogeneous and it consists of various sub-clones with different status of p53 gene as a result of tumor progression (41-43). This genetic heterogeneity in esophageal cancer may underlie the heterogeneous expression of the proteins mentioned above and that of DNA-PK proteins as reported in this study. Furthermore, the contribution of increased Sp1 activity to tumor progression has been reported (33). Upregulation of Sp1 in the process of tumor progression may increase the DNA-PK activity/protein levels of the tumor cells, as shown in Figs. 1, 2 and 6, and cause the acquisition of radioresistant phenotype.

In summary, DNA-PK activity was higher in the esophageal tumor tissues compared with the adjacent normal mucosae, and DNA-PK protein levels correlated with DNA-PK activity. Expression of DNA-PK proteins showed intratumoral heterogeneity in esophageal cancer tissues, making difficult the prediction of curability of the tumors after radiotherapy or chemotherapy by estimation of DNA-PK activity/protein levels in tumor specimens.

References

1. Gottlieb TM and Jackson SP: The DNA-dependent protein kinase: requirement for DNA ends and association with Ku antigen. Cell 72: 131-142, 1993.
2. Jeggo PA, Taccioli GE and Jackson SP: Menage a trois: double strand break repair, V(D)J recombination and DNA-PK. Bioessays 17: 949-957, 1995.
3. Lees-Miller SP, Godbout R, Chan DW, Weinfeld M, Day RS III, Barron GM and Allalunis-Turner J: Absence of p350 subunit of DNA-activated protein kinase from a radiosensitive human cell line. Science 267: 1183-1185, 1995.
4. Gu Y, Jin S, Gao Y, Weaver DT and Alt FW: Ku70-deficient embryonic stem cells have increased ionizing radiosensitivity, defective DNA end-binding activity, and inability to support V(D)J recombination. Proc Natl Acad Sci USA 94: 8076-8081, 1997.
5. Nussenzweig A, Sokol K, Burgman P, Li L and Li GC: Hypersensitivity of Ku80-deficient cell lines and mice to DNA damage: the effects of ionizing radiation on growth, survival, and development. Proc Natl Acad Sci USA 94: 13588-13593, 1997.
6. Gao Y, Chaudhuri J, Zhu C, Davidson L, Weaver DT and Alt FW: A targeted DNA-PKcs-null mutation reveals DNA-PK-independent functions for KU in V(D)J recombination. Immunity 9: 367-376, 1998.
7. Hosoi Y, Miyachi H, Matsumoto Y, Ikehata H, Komura J, Ishii K, Zhao HJ, Yoshida M, Takai Y, Yamada S, Suzuki N and Ono T: A phosphatidylinositol 3-kinase inhibitor wortmannin induces radioresistant DNA synthesis and sensitizes cells to bleomycin and ionizing radiation. Int J Cancer 78: 642-647, 1998.
8. Omori S, Takiguchi Y, Suda A, Sugimoto T, Miyazawa H, Takiguchi Y, Tanabe N, Tatsumi K, Kimura H, Pardington PE, Chen F, Chen DJ and Kuriyama T: Suppression of a DNA double-strand break repair gene, Ku70, increases radio- and chemosensitivity in a human lung carcinoma cell line. DNA Repair 1: 299-310, 2002.
9. Sak A, Stuschke M, Wurm R, Schroeder G, Sinn B, Wolf G and Budach V: Selective inactivation of DNA-dependent protein kinase with antisense oligodeoxynucleotides: consequences for the rejoining of radiation-induced DNA double-strand breaks and radiosensitivity of human cancer cell lines. Cancer Res 62: 6621-6624, 2002.
10. Collis SJ, Swartz MJ, Nelson WG and De Weese TL: Enhanced radiation and chemotherapy-mediated cell killing of human cancer cells by small inhibitory RNA silencing of DNA repair factors. Cancer Res 63: 1550-1554, 2003.
11. Polischouk AG, Cedervall B, Ljungquist S, Flygare J, Hellgren D, Grenman R and Lewensohn R: DNA double-strand break repair, DNA-PK, and DNA ligases in two human squamous carcinoma cell lines with different radiosensitivity. Int J Radiat Oncol Biol Phys 43: 191-198, 1999.
12. Allalunis-Turner MJ, Lintott LG, Barron GM, Day RS and Lees-Miller SP: Lack of correlation between DNA-dependent protein kinase activity and tumor cell radiosensitivity. Cancer Res 55: 5200-5202, 1995.
13. Kasten U, Plottner N, Johansen J, Overgaard J and Dikomey E: Ku70/80 gene expression and DNA-dependent protein kinase (DNA-PK) activity do not correlate with double-strand break (dsb) repair capacity and cellular radiosensitivity in normal human fibroblasts. Br J Cancer 79: 1037-1041, 1999.
14. Sirzen F, Nilsson A, Zhivotovsky B and Lewensohn R: DNA-dependent protein kinase content and activity in lung carcinoma cell lines: correlation with intrinsic radiosensitivity. Eur J Cancer 35: 111-116, 1999.
15. Vaganay-Juery S, Muller C, Marangoni E, Abdulkarim B, Deutsch E, Lambin P, Calsou P, Eschwege F, Salles B, Joiner M and Bourhis J: Decreased DNA-PK activity in human cancer cells exhibiting hypersensitivity to low-dose irradiation. Br J Cancer 83: 514-518, 2000.
16. Bjork-Eriksson T, West C, Nilsson A, Magnusson B, Svensson M, Karlsson E, Slevin N, Lewensohn R and Mercke C: The immunohistochemical expression of DNA-PKCS and Ku (p70/p80) in head and neck cancers: relationships with radiosensitivity. Int J Radiat Oncol Biol Phys 45: 1005-1010, 1999.
17. Zhao HJ, Hosoi Y, Miyachi H, Ishii K, Yoshida M, Nemoto K, Takai Y, Yamada S, Suzuki N and Ono T: DNA-dependent protein kinase activity correlates with Ku70 expression and radiation sensitivity in esophageal cancer cell lines. Clin Cancer Res 6: 1073-1078, 2000.
18. Wilson CR, Davidson SE, Margison GP, Jackson SP, Hendry JH and West CM: Expression of Ku70 correlates with survival in carcinoma of the cervix. Br J Cancer 83: 1702-1706, 2000.
19. Sakata K, Matsumoto Y, Tauchi H, Satoh M, Oouchi A, Nagakura H, Koito K, Hosoi Y, Suzuki N, Komatsu K and Hareyama M: Expression of genes involved in repair of DNA double-strand breaks in normal and tumor tissues. Int J Radiat Oncol Biol Phys 49: 161-167, 2001.

20. Komuro Y, Watanabe T, Hosoi Y, Matsumoto Y, Nakagawa K, Tsuno N, Kazama S, Kitayama J, Suzuki N and Nagawa H: The expression pattern of Ku correlates with tumor radiosensitivity and disease free survival in patients with rectal carcinoma. Cancer 95: 1199-1205, 2002.
21. Hosoi Y, Watanabe T, Nakagawa K, Matsumoto Y, Enomoto A, Morita A, Nagawa H and Suzuki N: Up-regulation of DNA-dependent protein kinase activity and Sp1 in colorectal cancer. Int J Oncol 25: 461-468, 2004.
22. Murnane JP: Inducible gene expression by DNA rearrangements in human cells. Mol Cell Biol 6: 549-558, 1986.
23. Finnie NJ, Gottlieb TM, Blunt T, Jeggo PA and Jackson SP: DNA-dependent protein kinase activity is absent in xrs-6 cells: implications for site-specific recombination and DNA double-strand break repair. Proc Natl Acad Sci USA 92: 320-324, 1995.
24. Dignam JD, Lebovitz RM and Roeder RG: Accurate transcription initiation by RNA polymerase II in a soluble extract from isolated mammalian nuclei. Nucleic Acids Res 11: 1475-1489, 1983.
25. Hosoi Y, Kawamura M, Ido T, Takai Y, Ishii K, Nemoto K, Ono T, Kimura S and Sakamoto K: Sensitization of cells to ionizing radiation by chlorin e6Na. Radiat Oncol Investig 6: 151-156, 1998.
26. Rigas B, Borgo S, Elhosseiny A, Balatsos V, Manika Z, Shinya H, Kurihara N, Go M and Lipkin M: Decreased expression of DNA-dependent protein kinase, a DNA repair protein, during human colon carcinogenesis. Cancer Res 61: 8381-8384, 2001.
27. Chino O, Makuuchi H, Shimada H, Machimura T, Mitomi T and Osamura RY: Assessment of the proliferative activity of superficial esophageal carcinoma using MIB-1 immunostaining for the Ki-67 antigen. J Surg Oncol 67: 18-24, 1998.
28. Yoshida M, Hosoi Y, Miyachi H, Ishii N, Matsumoto Y, Enomoto A, Nakagawa K, Yamada S, Suzuki N and Ono T: Roles of DNA-dependent protein kinase and ATM in cell-cycle-dependent radiation sensitivity in human cells. Int J Radiat Biol 78: 503-512, 2002.
29. Ludwig DL, Chen F, Peterson SR, Nussenzweig A, Li GC and Chen DJ: Ku80 gene expression is Sp1-dependent and sensitive to CpG methylation within a novel cis element. Gene 199: 181-194, 1997.
30. Fujimoto M, Matsumoto N, Tsujita T, Tomita H, Kondo S, Miyake N, Nakano M and Niikawa N: Characterization of the promoter region, first ten exons and nine intron-exon boundaries of the DNA-dependent protein kinase catalytic subunit gene, DNA-PKcs (XRCC7). DNA Res 4: 151-154, 1997.
31. Milanini J, Vinals F, Pouyssegur J and Pages G: p42/p44 MAP kinase module plays a key role in the transcriptional regulation of the vascular endothelial growth factor gene in fibroblasts. J Biol Chem 273: 18165-18172, 1998.
32. Kutoh E, Margot JB and Schwander J: Identification and characterization of the putative retinoblastoma control element of the rat insulin-like growth factor binding protein-2 gene. Cancer Lett 136: 187-194, 1999.
33. Ishibashi H, Nakagawa K, Onimaru M, Castellanous EJ, Kaneda Y, Nakashima Y, Shirasuna K and Sueishi K: Sp1 decoy transfected to carcinoma cells suppresses the expression of vascular endothelial growth factor, transforming growth factor beta1, and tissue factor and also cell growth and invasion activities. Cancer Res 60: 6531-6536, 2000.
34. Saeki H, Kuwano H, Kawaguchi H, Ohno S and Sugimachi K: Expression of ets-1 transcription factor is correlated with penetrating tumor progression in patients with squamous cell carcinoma of the esophagus. Cancer 89: 1670-1676, 2000.
35. Murakami H, Furihata M, Ohtsuki Y and Ogoshi S: Determination of the prognostic significance of cyclin B1 overexpression in patients with esophageal squamous cell carcinoma. Virchows Arch 434: 153-158, 1999.
36. Ishikawa T, Furihata M, Ohtsuki Y, Murakami H, Inoue A and Ogoshi S: Cyclin D1 overexpression related to retinoblastoma protein expression as a prognostic marker in human oesophageal squamous cell carcinoma. Br J Cancer 77: 92-97, 1998.
37. Xing EP, Yang GY, Wang LD, Shi ST and Yang CS: Loss of heterozygosity of the Rb gene correlates with pRb protein expression and associates with p53 alteration in human esophageal cancer. Clin Cancer Res 5: 1231-1240, 1999.
38. Abdalla SI, Sanderson IR and Fitzgerald RC: Effect of inflammation on cyclooxygenase (COX)-2 expression in benign and malignant oesophageal cells. Carcinogenesis 26: 1627-1633, 2005.
39. Akcakanat A, Kanda T, Tanabe T, Komukai S, Yajima K, Nakagawa S, Ohashi M and Hatakeyama K: Heterogeneous expression of GAGE, NY-ESO-1, MAGE-A and SSX proteins in esophageal cancer: Implications for immunotherapy. Int J Cancer 118: 123-128, 2006.
40. Kadowaki T, Shiozaki H, Inoue M, Tamura S, Oka H, Doki Y, Iihara K, Matsui S, Iwazawa T and Nagafuchi A: E-cadherin and alpha-catenin expression in human esophageal cancer. Cancer Res 54: 291-296, 1994.
41. Kaketani K, Saito T, Kuwahara A, Shimoda K, Miyahara M, Chikuba K, Etoh K and Kobayashi M: DNA stem line heterogeneity in esophageal cancer accurately identified by flow cytometric analysis. Cancer 72: 3564-3570, 1993.
42. Kuwabara S, Ajioka Y, Watanabe H, Hitomi J, Nishikura K and Hatakeyama K: Heterogeneity of p53 mutational status in esophageal squamous cell carcinoma. Jpn J Cancer Res 89: 405-410, 1998.
43. Shi ST, Yang GY, Wang LD, Xue Z, Feng B, Ding W, Xing EP and Yang CS: Role of p53 gene mutations in human esophageal carcinogenesis: results from immunohistochemical and mutation analyses of carcinomas and nearby non-cancerous lesions. Carcinogenesis 20: 591-597, 1999.

Haploinsufficiency of *RAD51B* Causes Centrosome Fragmentation and Aneuploidy in Human Cells

Osamu Date,[1,2] Mari Katsura,[1] Mari Ishida,[1] Takashi Yoshihara,[1] Aiko Kinomura,[1] Taijiro Sueda,[2] and Kiyoshi Miyagawa[1,3]

[1]Department of Human Genetics, Research Institute for Radiation Biology and Medicine and [2]Department of Surgery, Graduate School of Medical Sciences, Hiroshima University, Hiroshima, Japan and [3]Section of Radiation Biology, Graduate School of Medicine, The University of Tokyo, Tokyo, Japan

Abstract

The Rad51-like proteins, Rad51B, Rad51C, Rad51D, XRCC2, and XRCC3, have been shown to form two distinct complexes and seem to assist Rad51 in the early stages of homologous recombination. Although these proteins share sequence similarity with Rad51, they do not show functional redundancy. Among them, Rad51B is unique in that the gene maps to the human chromosome 14q23-24, the region frequently involved in balanced chromosome translocations in benign tumors particularly in uterine leiomyomas. Despite accumulating descriptive evidence of altered Rad51B function in these tumors, the biological significance of this aberration is still unknown. To assess the significance of reduced Rad51B function, we deleted the gene in the human colon cancer cell line HCT116 by gene targeting. Here, we show that haploinsufficiency of *RAD51B* causes mild hypersensitivity to DNA-damaging agents, a mild reduction in sister chromatid exchange, impaired Rad51 focus formation, and an increase in chromosome aberrations. Remarkably, haploinsufficiency of *RAD51B* leads to centrosome fragmentation and aneuploidy. In addition, an ~50% reduction in *RAD51B* mRNA levels by RNA interference also leads to centrosome fragmentation in the human fibrosarcoma cell line HT1080. These findings suggest that the proper biallelic expression of *RAD51B* is required for the maintenance of chromosome integrity in human cells. (Cancer Res 2006; 66(12): 6018-24)

Introduction

The centrosome is the primary microtubule-organizing center in vertebrate cells and forms the poles of the mitotic spindles that facilitate chromosome segregation (1). A direct link between centrosome abnormalities and chromosome instability has been suggested by the significant correlation between centrosome amplification and aneuploidy in human cancers (2, 3). Inactivation of tumor suppressor genes or amplification of oncogenes also induces centrosome amplification and aneuploidy in mammals (4–7). Such correlations have led to the hypothesis that centrosome amplification plays a causal role in chromosome instability.

DNA double-strand breaks (DSB) are repaired either by nonhomologous end joining or homologous recombination (8, 9). Rad51 promotes homologous DNA pairing and strand exchange, thereby playing a central role in the early stages of homologous recombination (10). Defects in homologous recombination repair have been shown to cause centrosome abnormalities. An increase in the number of centrosomes has been observed in rodent and chicken cells deficient in BRCA1, BRCA2, Mre11, XRCC2, XRCC3, Rad51, or Rad51D (6, 11–15). It should be noted that the increases in centrosome numbers in cells deficient in BRCA1, BRCA2, Mre11, or Rad51 have resulted from centrosome amplification, whereas such increases in cells deficient in other proteins have resulted from centrosome fragmentation. Consequently, the frequency of aneuploidy has been found to be increased in rodent cells deficient in BRCA1, BRCA2, XRCC2, or XRCC3. It has been reported that BRCA1 is localized at the centrosome (16). In addition, ataxia-telangiectasia mutated (ATM) is involved in centrosome amplification in Rad51-deficient DT40 cells (14). Despite these observations, the primary causes for these aberrations have not been fully characterized.

Rad51B (Rad51L1), a member of the Rad51 paralogue family, plays a role in homologous recombination in concert with Rad51 and other Rad51 paralogues by directly associating with Rad51C (17–19). Additionally, biochemical evidence that Rad51B binds to the Holliday junction has suggested that the protein may play a role in the late phase of homologous recombination (20). Consistent with this finding, Rad51C or Rad51C-associated proteins have been proposed to be components of Holliday junction resolvase (21), although there is not yet any direct evidence that Rad51B is involved in the resolution of recombination intermediates. Cellular functions of Rad51B have been investigated in chicken DT40 cells. Hypersensitivity to DNA-damaging agents, decreases in sister chromatid exchange (SCE) and gene targeting, impaired damage-dependent Rad51 focus formation, and an increase in chromosome aberrations have been observed in *RAD51B*$^{-/-}$ DT40 cells (22). Although Chinese hamster ovary (CHO) cells have been used for the functional analysis of XRCC2, XRCC3, and Rad51C, CHO cells deficient in Rad51B have not been available thus far. *RAD51B*$^{-/-}$ mice die in the early embryonic stages, suggesting that Rad51B plays a role in development (23).

An interesting feature of Rad51B in cancer genetics is that the gene maps to the chromosome break point in some benign tumors that harbor balanced chromosome translocations involving 14q23-24 (24). The involvement of Rad51B in benign tumors was first found in uterine leiomyomas harboring a balanced chromosome translocation between chromosomes 12 and 14 with the high mobility group protein HMGA2 (HMGIC) as the partner (25, 26). Chimeric transcripts encoding either *RAD51L1/HMGA2* or *HMGA2/RAD51L1* have been found in some uterine leiomyomas (25, 27, 28). In pseudo-Meigs' syndrome, which is characterized by uterine leiomyomas, ascites, and pleural effusion, a combination of the *HMGA2/RAD51L1* fusion and a loss of the second *RAD51L1* allele were observed (29). In addition, *RAD51B* is involved in other types

Requests for reprints: Kiyoshi Miyagawa, Section of Radiation Biology, Graduate School of Medicine, The University of Tokyo, 7-3-1 Hongo, Bunkyo-ku, Tokyo 113-0033, Japan. Phone: 81-3-5841-3503; Fax: 81-3-5841-3013; E-mail: miyag-tky@umin.ac.jp.

doi:10.1158/0008-5472.CAN-05-2803

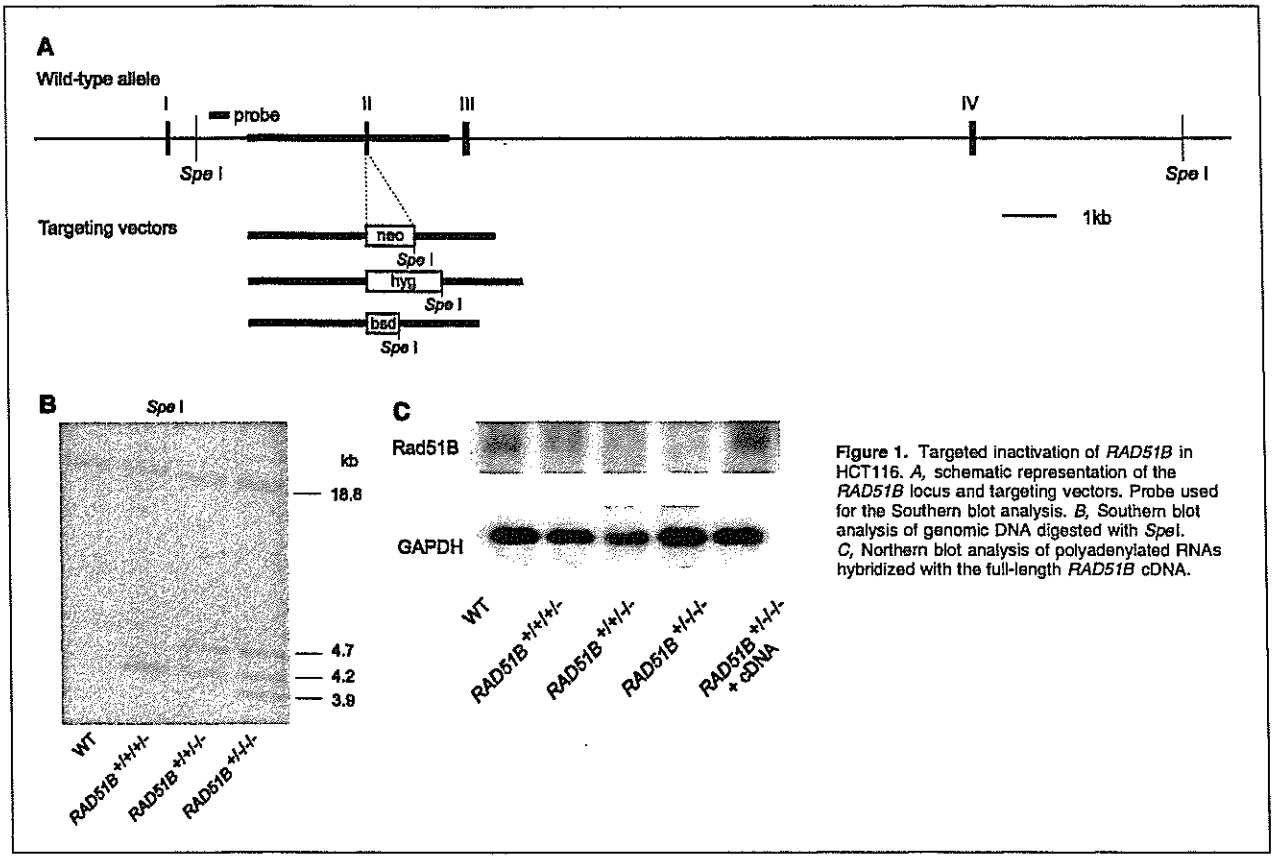

Figure 1. Targeted inactivation of *RAD51B* in HCT116. *A*, schematic representation of the *RAD51B* locus and targeting vectors. Probe used for the Southern blot analysis. *B*, Southern blot analysis of genomic DNA digested with *SpeI*. *C*, Northern blot analysis of polyadenylated RNAs hybridized with the full-length *RAD51B* cDNA.

of balanced chromosome translocations in pulmonary chondroid hamartomas (30) and thymomas (31). These studies indicate that at least one allele of *RAD51B* is altered in some benign tumors, but the key pathologic event is still unclear. For this reason, the elucidation of the significance of *RAD51B* haploinsufficiency has been awaited.

To investigate the putative role of Rad51B in human cells, we sequentially knocked out the gene by gene targeting in the human colon cancer cell line HCT116. Here, we show that haploinsufficiency of *RAD51B* leads to a defect in homologous recombination repair as well as to centrosome fragmentation and increased aneuploidy. A reduction in *RAD51B* levels by RNA interference (RNAi) also leads to centrosome fragmentation in the human fibrosarcoma cell line HT1080. Thus, a loss of the proper biallelic expression of *RAD51B* leads to chromosome instability by preventing centrosome integrity in human tumor cells.

Materials and Methods

Targeted inactivation of the *RAD51B* gene. Targeting vectors were designed to insert promoterless drug resistance genes in exon 2 in the frame. A 2.2-kb 5′ homology arm was amplified from the isogenic DNA of HCT116 cells using the primers 5′-TAAGGCAGAAATGGCAGA-3′ and 5′-TATCGATGTTTCTTGCTACCCAT-3′. A 1.6-kb 3′ homology arm was amplified using the primers 5′-ATAGCTAAAGAGCTGTGTGACCG-3′ and 5′-TACTAGTATGAGCGCTACACTTG-3′. Both arms were cloned into pCR2.1 (Invitrogen, Carlsbad, CA) by the TA cloning method. The 3′ arm was cut out with *Spe*I digestion and subcloned into the vector containing the 5′ arm. Neomycin, hygromycin, and blasticidin resistance genes were inserted into the *Cla*I site of the vector containing homology arms. Gene targeting in HCT116 was done as described previously (32).

Ectopic expression of the *RAD51B* cDNA. The human *RAD51B* cDNA was amplified from cDNA derived from normal human cells using the primers 5′-CGCGGGGAAACTGTGTAAA-3′ and 5′-GGCAAGATGAA-CAGGTTTGC-3′. The cDNA was cloned into pCR2.1, and the sequence was confirmed. The expression vector was designed to insert the *RAD51B* cDNA under the control of the murine sarcoma virus enhancer and the mouse mammary tumor virus promoter. The transfected cells were selected in the presence of 900 μg/mL Zeocin (Invitrogen).

Growth rate and sensitivity to DNA-damaging agents. To measure growth rate, the cells were plated at a density of 10^4 per 60-mm dish and cultured. The cells were counted on the days indicated. To measure sensitivity to DNA damage, the cells were irradiated with a ^{60}Co source or treated with mitomycin C (MMC; Kyowa Hakko, Tokyo, Japan) in suspension for 10 minutes and plated at a density of 2×10^3 per 60-mm dish. After 7 days of culturing, the colonies of wild-type (WT) cells were counted. Because knockout and complemented cells grew more slowly than WT cells, we factored growth rate into the counting of colonies; the colonies of these cells were further cultured and counted after 9 to 10 days.

SCE and gene targeting. The frequency of SCEs was measured essentially as described previously (32). Wild-type cells were cultured in 16 μmol/L 5-bromodeoxyuridine for 32 hours. Because the mutant showed slow growth, *RAD51B*$^{+/-/-/-}$ and the cDNA-expressing cells were cultured in the agent for 40 and 36 hours, respectively. To examine MMC-induced SCE, the cells were incubated in the presence of 0.8 μg/mL MMC for 8 hours. The gene-targeting frequency was examined using *RAD54B-hyg* and *RAD51C-pur* vectors (32).

Antibodies. We used commercially available antibodies to Rad51 from Oncogene Research (San Diego, CA) and to γ-tubulin and β-tubulin from Sigma (St. Louis, MO).

Immunostaining. The cells were cultured on glass slides, fixed in ice-cold methanol for 10 minutes, washed in PBS, and blocked in fetal bovine serum for 15 minutes. Rad51 focus formation was examined as described previously (33). The cells were either nontreated or irradiated with 8 Gy and stained at 2.5 hours after irradiation with anti-Rad51 antibody. The cells were also treated with 0.8 μg/mL MMC for 1 hour and stained at 2 hours after treatment. Centrosomes were detected by anti-γ-tubulin antibody. Microtubules were detected by anti-β-tubulin antibody. The cells were counterstained with 4′,6-diamidino-2-phenylindole.

Fluorescence *in situ* hybridization analysis. Chromosome-specific centromere probes were obtained from Vysis (Downers Grove, IL). Hybridization was done according to the manufacturer's protocol.

Small interfering RNA transfection. To knock down Rad51B in stably transformed cells, a DNA fragment flanked by the *Bam*HI and *Hin*dIII sites containing the sense target sequence (5′-AGCACAAAGGTCTGCTGAT-3′), the hairpin loop sequence (5′-TTCAAGAGA-3′), and the antisense target sequence was synthesized and inserted into pBAsi-hU6 Neo (Takara, Otsu, Japan). Similarly, the control sequence (5′-TAGCGACTAAACACATCAA-3′) was used to construct the vector used for a negative control. Transfected cells were selected in the presence of 400 μg/mL G418.

Real-time reverse transcription-PCR. Total RNA was extracted from cytoplasm (34). Total RNA (500 ng) was reverse transcribed in a total of 20 μL reaction mixture. Real-time PCR was carried out with the ABI Prism 7700 sequence detection system (Applied Biosystems, Foster City, CA) in a 20-μL reaction volume containing 1 μL cDNA using SYBR Green (Qiagen, Valencia, CA) for the detection of PCR products. The PCR primers were as follows: *RAD51B*, 5′-CAGTGTGAATACCCGGCTGA-3′ and 5′-CTTGATGGTGTAGACAAATGAGGTG-3′ and glyceraldehyde-3-phosphate dehydrogenase (GAPDH), 5′-GCACCGTCAAGGCTGAGAAC-3′ and 5′-ATGGTGGTGAAGACGCCAGT-3′. The expression level of the *RAD51B* gene was evaluated as the ratio of its mRNA to that of *GAPDH* mRNA.

Results

Rad51B is required for gene targeting. The *RAD51B* gene was sequentially knocked out by gene targeting in the HCT116 cell line (Fig. 1*A*). Southern blot analysis revealed that this cell line harbors four *RAD51B* alleles (Fig. 1*B*). Rad51B-null cells were not generated because the targeting frequencies in the triple knockout cells were extremely low. The effect of the triple knockout on gene targeting was examined at two independent loci (32). The frequency at the *RAD54B* locus was 6.1% (25 of 407) in WT cells, whereas it was 1.4% (2 of 141) in $RAD51B^{+/-/-/-}$ cells. Similarly, the frequencies at the *RAD51C* locus were 0.3% (12 of 3,985) in WT cells and 0% (0 of 1,436) in $RAD51B^{+/-/-/-}$ cells. These differences were statistically significant ($P < 0.05$, Fisher's exact test). In addition, the frequencies in $RAD51B^{+/+/-/-}$ cells were 5.6% (4 of 72) at the *RAD54B* locus and 0.33% (4 of 1,216) at the *RAD51C* locus, indicating a difference in gene-targeting frequency between $RAD51B^{+/+/-/-}$ and $RAD51B^{+/-/-/-}$ cells. This finding suggests that Rad51B is required for gene targeting in human cells; thus, the present results are in accord with those of a previous report using chicken DT40 cells (22). Northern blot analysis confirmed that the expression levels correlated well with the targeting events; the level of Rad51B in $RAD51B^{+/-/-/-}$ cells was approximately one fourth that of the WT cells (Fig. 1*C*). The level of Rad51B by ectopic expression was almost identical to that in WT cells. We then investigated Rad51B function using the $RAD51B^{+/-/-/-}$ cell line.

Growth and sensitivity to DNA-damaging agents of *rad51b*-mutant cells. The *rad51b*-mutant cells grew at a slightly slower rate than the WT cells, with a doubling time of 21 hours versus 16 hours (Fig. 2*A*). We next examined the sensitivity of *rad51b*-mutant cells to DNA damage by measuring their ability to form colonies following exposure to DNA-damaging agents. The *rad51b*-mutant exhibited mild hypersensitivity to γ-irradiation (2-fold; Fig. 2*B*). The mutant cells also exhibited mild hypersensitivity to the DNA interstrand cross-linking agent MMC (2.5-fold; Fig. 2*C*). The expression of the transfected cDNA partially complemented this phenotype. Thus, the present findings suggest that Rad51B plays a role in DNA DSB repair.

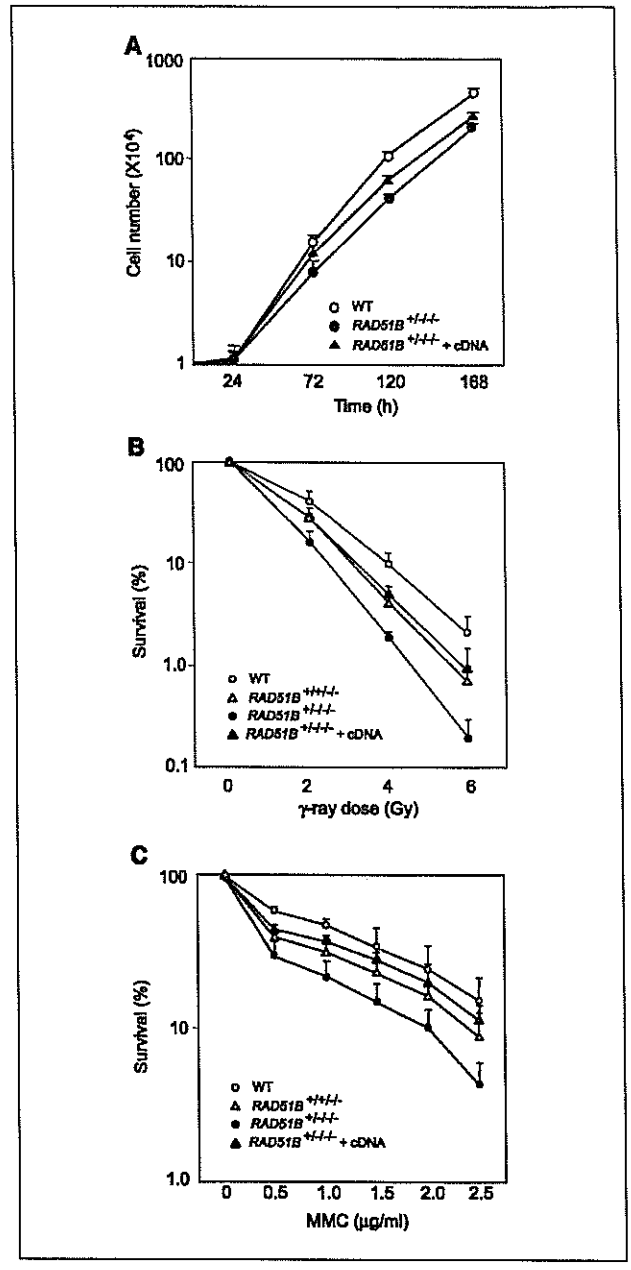

Figure 2. Growth and sensitivity to DNA damage of *rad51b*-mutant cells. *A*, growth curves. *B*, sensitivity to γ-irradiation. *C*, sensitivity to MMC. *Points*, mean of three independent experiments; *bars*, SD.

Rad51B is involved in SCE. Lower levels of SCE have been found in cells deficient in homologous recombination repair (35). In the present study, the frequencies of spontaneous SCEs were 4.3 ± 1.8 (mean ± SD) in WT cells (n = 131) and 3.4 ± 1.5 in *rad51b*-mutant cells (n = 116; Fig. 3*A*). Despite a small frequency reduction in the mutant cells, this difference was statistically significant (P < 0.001, Mann-Whitney U test). The frequencies of MMC-induced SCEs were 8.3 ± 3.9 in WT cells (n = 98) and 6.7 ± 3.6 in mutant cells (n = 120). This difference was also statistically significant (P < 0.001). The expression of the *RAD51B* cDNA increased the frequencies of SCEs to the WT levels. These findings suggest that Rad51B is involved in homologous recombination by using sister chromatids.

***RAD51B* haploinsufficiency impairs Rad51 focus formation.** DNA damage induces the formation of Rad51 foci in the nucleus (33). A decrease in Rad51 focus formation has been observed in cells deficient in genes that are involved in the early stages of homologous recombination in concert with Rad51 (36–38). We therefore examined damage-dependent focus formation of Rad51 in the *rad51b*-mutant cells (Fig. 3*B*). Because many cells contained one to five foci even in the absence of DNA damage, a cell containing more than five foci was scored as positive. The percentage of positive cells after irradiation was 73.7 ± 5.1% (mean ± SD) among WT cells, 64.7 ± 4.7% among *RAD51B*$^{+/+/-/-}$ cells, and 50.7 ± 5.9% among *RAD51B*$^{+/-/-/-}$ cells (Fig. 3*C*). The expression of *RAD51B* in *RAD51B*$^{+/-/-/-}$ cells increased the percentage to 73 ± 4.6%. Similarly, the percentage of positive cells after MMC treatment was 64.7 ± 1.4% among WT cells, 46 ± 8.1% among *RAD51B*$^{+/+/-/-}$ cells, and 37.3 ± 1.4% among *RAD51B*$^{+/-/-/-}$ cells (Fig. 3*C*). The expression of *RAD51B* in *RAD51B*$^{+/-/-/-}$ cells increased the percentage to 60.7 ± 2%. These findings suggest that Rad51B is required for the recruitment of Rad51 to damaged sites in the nucleus.

Rad51B is required for chromosome stability. Because a defect in homologous recombination has been shown to promote chromosome aberrations (39), we did chromosome analysis by preparing metaphase spreads in the presence of colcemid. Spontaneous chromatid-type and chromosome-type aberrations, including gaps, breaks, and exchanges, were significantly (8-fold) increased in *rad51b*-mutant cells (Fig. 3*D*). This chromosome damage was reduced by the expression of the *RAD51B* cDNA. These findings suggest that Rad51B is required for the maintenance of chromosome stability in human cells.

***RAD51B* haploinsufficiency leads to centrosome fragmentation.** We next examined centrosome aberrations by immunostaining γ-tubulin because centrosome fragmentation has been observed in other mutant cells deficient in XRCC2, XRCC3, or Rad51D (13, 15). In the *rad51b* mutant, cells with multiple centrosomes were more frequently observed (Fig. 4*A* and *B*). The presence of smaller centrosome-like structures indicated that these numerous abnormalities were caused by centrosome fragmentation rather than by centrosome amplification. The frequency of aberrant numbers of interface centrosomes (more than two) was 5% in WT cells, whereas it was 11.5% in *RAD51B*$^{+/+/-/-}$ cells and

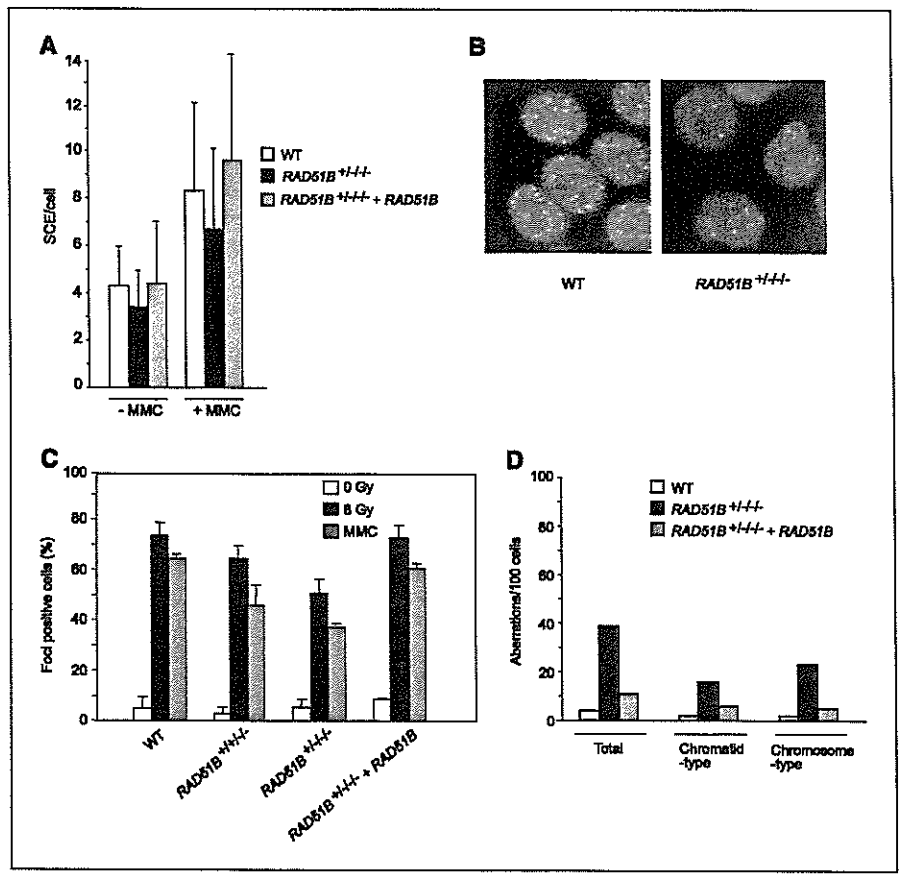

Figure 3. Rad51B plays a role in the Rad51-dependent recombination repair pathway. *A*, frequency of SCEs. *Columns*, mean from at least 98 mitotic cells; *bars*, SD. *B*, damage-dependent Rad51 focus formation. The cells were treated with 0.8 μg/mL MMC for 1 hour and stained at 2 hours after treatment. *C*, decreased levels of damage-dependent Rad51 focus formation. Percentage of cells containing more than five damage-induced Rad51 foci. *Columns*, mean of three independent experiments; *bars*, SD. A total of 100 cells were examined for each cell line. *D*, spontaneous chromosome aberrations in the absence of DNA-damaging agents. Data are the numbers of aberrations per 100 cells. A total of 100 mitotic cells were examined for each cell line.

14% in *RAD51B*$^{+/-/-/-}$ cells (Table 1). The expression of the *RAD51B* cDNA in the mutant reduced the frequency of such aberrations to 5%. Similarly, in metaphase, the frequency was 6% in WT cells, 13.5% in *RAD51B*$^{+/+/-/-}$ cells, and 25.5% in *RAD51B*$^{+/-/-/-}$ cells. The expression of the *RAD51B* cDNA in the mutant reduced the frequency to 10.5%. Thus, haploinsufficiency of *RAD51B* leads to increased centrosome fragmentation.

***RAD51B* haploinsufficiency leads to increased aneuploidy.** Extra centrosome-like structures can unequally distribute chromosomes to daughter cells, which is thought to cause aneuploidy. We therefore examined the frequency of aneuploidy by fluorescence *in situ* hybridization (FISH) using two independent chromosome-specific centromere probes (Fig. 4*C*; Table 2). At chromosome 7, the frequencies of aneuploidy represented by one or three signals were 5.4% in WT cells, whereas the corresponding frequency was 9.8% in *RAD51B*$^{+/+/-/-}$ cells and 14% in *RAD51B*$^{+/-/-/-}$ cells. At chromosome 17, the frequencies of aneuploidy were 3.8% in WT cells, whereas the corresponding frequency was 7.4% in *RAD51B*$^{+/+/-/-}$ cells and 10.2% in *RAD51B*$^{+/-/-/-}$ cells. The differences between WT cells and the mutant cells were statistically significant ($P < 0.05$, Fisher's exact test). Expression of the *RAD51B* cDNA in the mutant reduced the frequency of aneuploidy to 6.4% at chromosome 7 and 4.2% at chromosome 17 ($P < 0.05$). Thus, haploinsufficiency of *RAD51B* leads to increased aneuploidy.

It is possible that *RAD51B*$^{+/-/-/-}$ cells will acquire more copies of the WT allele and form significant subpopulations due to increased aneuploidy. To investigate this possibility, we examined a difference in *RAD51B* expression levels between originally isolated cells and cells passaged 25 times by Northern blot analysis and found no difference. Thus, despite the problem of chromosome segregation, the *RAD51B*$^{+/-/-/-}$ status is stable.

Table 1. Distribution of centrosome numbers

Cell line	1 or 2	3	4	>4	% Abnormality
Interphase					
HCT116					
RAD51B$^{+/+/+/+}$	190	8	2	0	5
RAD51B$^{+/+/-/-}$	177	15	7	1	11.5
RAD51B$^{+/-/-/-}$	172	22	4	2	14
RAD51B$^{+/-/-/-}$ + *RAD51B*	190	8	1	1	5
HT1080					
Control siRNA	197	1	2	0	1.5
RAD51B siRNA	192	6	2	0	4
Metaphase					
HCT116					
RAD51B$^{+/+/+/+}$	188	11	1	0	6
RAD51B$^{+/+/-/-}$	173	22	4	1	13.5
RAD51B$^{+/-/-/-}$	149	41	10	0	25.5
RAD51B$^{+/-/-/-}$ + *RAD51B*	179	19	2	0	10.5
HT1080					
Control siRNA	195	3	2	0	2.5
RAD51B siRNA	167	26	7	0	16.5

NOTE: A total of 200 cells were scored for each line.

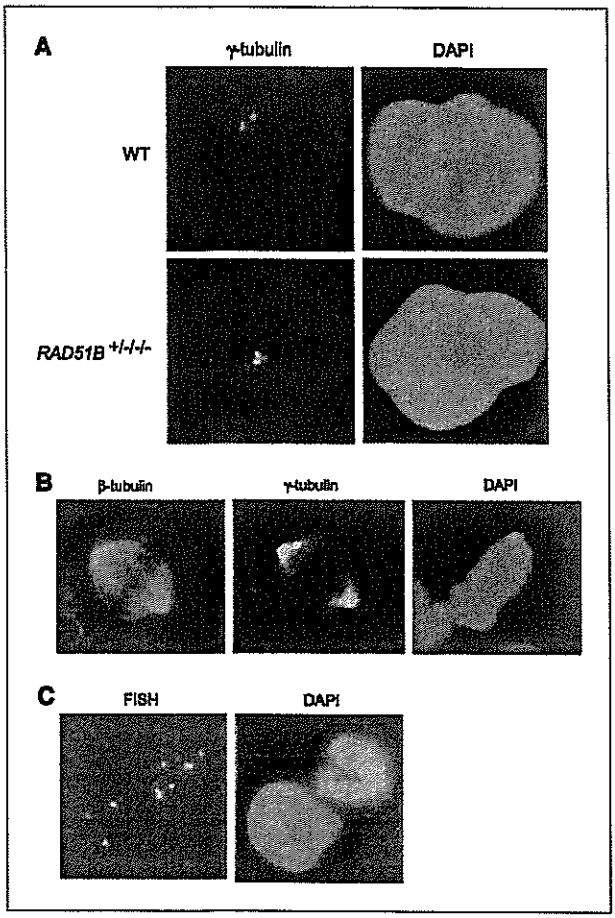

Figure 4. Centrosome fragmentation and aneuploidy in the *rad51b*-mutant cells. *A*, interphase *RAD51B*$^{+/-/-/-}$ cell with multiple centrosomes. *DAPI*, 4′,6-diamidino-2-phenylindole. *B*, metaphase *RAD51B*$^{+/-/-/-}$ cell showing multiple centrosomes and bipolar spindles. *C*, FISH on *RAD51B*$^{+/-/-/-}$ cells using a probe for chromosome 7 (*orange*) and a probe for chromosome 17 (*green*).

A reduction in *RAD51B* levels leads to centrosome fragmentation in HT1080 cells. To confirm that a reduction in *RAD51B* levels leads to centrosome fragmentation in other human cells, we knocked down the gene in HT1080 cells by small interfering RNA (siRNA) transfection. Real-time PCR analysis revealed that the mRNA ratio of *RAD51B*/*GAPDH* was $2.5 \pm 0.6 \times 10^{-4}$ (mean ± SD; $n = 3$) in cells transfected with a control vector, whereas it was $1.2 \pm 0.1 \times 10^{-4}$ in cells transfected with a Rad51B knockdown vector. Thus, an ~50% reduction in *RAD51B* mRNA levels was achieved by RNAi. The frequency of aberrant numbers of interface centrosomes was 1.5% in cells transfected with the control vector, whereas it was 4% in cells transfected with the *RAD51B* knockdown vector (Table 1). In metaphase, the frequency was 2.5% in the control cells and 16.5% in *RAD51B* knockdown cells. Thus, like the haploinsufficiency of *RAD51B* in HCT116 cells, the 50% reduction in *RAD51B* mRNA levels in HT1080 cells leads to centrosome fragmentation.

Discussion

In the present study, we have shown that haploinsufficiency of *RAD51B* leads to centrosome fragmentation and increased aneuploidy in the human cancer cell line HCT116. In addition,

we have confirmed that Rad51B plays a role in homologous recombination repair in concert with Rad51 in human cells, which is consistent with the previous finding in DT40 cells (22). However, the absence of *RAD51B* haploinsufficiency in knockout mice and DT40 mutants may argue against this interpretation of the findings (22, 23). This apparent discrepancy may be the result of species differences and/or differences between cell types. One finding of the present study, that a 50% reduction in *RAD51B* mRNA levels by RNAi in HT1080 cells also leads to centrosome fragmentation, suggests that the effects of *RAD51B* haploinsufficiency may not be specific to HCT116 cells. Furthermore, the present findings are also supported by evidence of haploinsufficiency for *XRCC2* in mouse cells (40). *XRCC2*$^{+/-}$ mice and *XRCC2*$^{+/-}$ DT40 cells have been shown to exhibit no apparent abnormalities (37, 41), whereas haploinsufficiency for the gene was clearly observed in chromosome aberrations and centrosome fragmentation in *XRCC2*$^{+/-}$ mouse embryonic fibroblasts. Rad51B forms a complex with Rad51C, Rad51D, and XRCC2 (BCDX2), suggesting a functional similarity between these Rad51 paralogues (42, 43). These subtle effects of haploinsufficiency on genomic instability, even if they are much weaker than the effects of homozygous mutations, are likely to be of considerable importance in carcinogenesis when they confer a growth advantage.

Although centrosome aberrations have been observed in cells defective in other recombination genes, the molecular mechanisms underlying these aberrations are unclear. Centrosome amplification has been shown to arise from a DNA damage-induced mechanism during the prolonged G_2 phase in Rad51-deficient DT40 cells (14). Deletion of ATM reduced, but did not completely abolish, G_2-phase centrosome amplification, thus indicating ATM-dependent and ATM-independent mechanisms. However, a recent study using CHO cells argues against this interpretation (44).

Centrosome aberrations found in cells deficient in a member of the Rad51 paralogue family seem to be centrosome fragmentations (13, 15). A recent observation has indicated that centrosomes split into fractions containing only one centriole, which leads to the formation of multipolar spindles with extra centrosome-like structures in the presence of incompletely replicated or damaged DNA during mitosis (45). This result is also observed in CHO cells deficient in XRCC3, suggesting that aneuploidy in this cell line arises from extra centrosome-like structures. It is therefore possible that centrosome fragmentation resulting from haploinsufficiency of *RAD51B* could be explained by centrosome splitting.

Aneuploidy is a hallmark of genetic instability observed in human cancers, although the direct cause remains a matter of debate (46). Extra centrosome-like structures are likely to lead to the assembly of multipolar spindles, which may in turn lead to the unequal distribution of chromosomes to daughter cells. However, supernumerary centrosomes do not always result in multipolarity, as shown by a recent finding that dynein plays a role in the prevention of multipolar spindles by centrosomal clustering (47). Consistent with this finding, multipolar spindles are rarely detected in the *rad51b* mutant, despite the increase in the incidence of supernumerary centrosomes. It is therefore unlikely that multipolar spindles play a causal role in increased aneuploidy in this mutant. This raises the question of how supernumerary centrosomes lead to aneuploidy. A possible clue may come from the characterization of the practical consequences of centrosome amplification in *p53*$^{-/-}$ mouse embryo fibroblasts (48, 49). In cells with two centrosomes at one spindle pole, a small fraction of chromosomes can be bioriented between incompletely separated centrosomes. Although these cells may divide in a bipolar fashion, this abnormal mitosis is likely to lead to the loss or gain of a few chromosomes.

From the viewpoint of tumor biology, it is of great importance that at least one allele of *RAD51B* is altered in some benign tumors, although the key pathologic alteration is still unclear. It is noteworthy that functional domains of Rad51B, such as Walker A and B motifs, are often lost as a consequence of the chromosome translocation, in contrast to the translocation partner HMGA2, the coding region of which is not rearranged by the translocation (28). It is well established that benign tumors do not usually develop into malignant tumors. However, a small proportion of benign tumors transforms into malignant tumors; <1% of uterine leiomyomas progress into uterine sarcomas. Given that the chromosome translocation involving *RAD51B* results in the loss of one functional *RAD51B* allele, the present finding that haploinsufficiency of the gene leads to aneuploidy implies chromosome instability in tumors harboring these translocations. The present study indicates that *rad51b*-mutant cells grow at a slightly slower rate than WT cells, implying that centrosome fragmentation and aneuploidy are not directly linked to a growth advantage. Aneuploidy is likely to contribute to a growth advantage only when genes that control cell growth are altered by the accumulation of chromosome instabilities. These observations lead to the hypothesis that the haploinsufficiency of *RAD51B*, even if not directly linked to malignant transformation, may play a role in the early steps of tumor development by inducing chromosome instability. To verify this hypothesis, a detailed analysis of *RAD51B* in association with pathologic and clinical studies in tumors involving 14q23-24 will be needed.

Table 2. Distribution of chromosome numbers

Cell line	1	2	3	4	>4	1 + 3
Chromosome 7						
RAD51B$^{+/+/+}$	17	469	10	4	0	27
RAD51B$^{+/+/-}$	27	442	22	8	1	49
RAD51B$^{+/-/-}$	52	419	18	9	2	70
RAD51B$^{+/-/-}$ + *RAD51B*	18	465	14	3	0	32
Chromosome 17						
RAD51B$^{+/+/+}$	16	476	3	5	0	19
RAD51B$^{+/+/-}$	23	452	14	10	1	37
RAD51B$^{+/-/-}$	37	439	14	9	1	51
RAD51B$^{+/-/-}$ + *RAD51B*	17	478	4	1	0	21

NOTE: A total of 500 cells were scored for each line.

Acknowledgments

Received 8/8/2005; revised 3/16/2006; accepted 4/13/2006.

Grant support: Ministry of Education, Culture, Sports, Science, and Technology of Japan; Ministry of Health, Labour, and Welfare of Japan; and Hiroshima University 21st Century Center of Excellence Program (M. Katsura and T. Yoshihara).

The costs of publication of this article were defrayed in part by the payment of page charges. This article must therefore be hereby marked *advertisement* in accordance with 18 U.S.C. Section 1734 solely to indicate this fact.

References

1. Delattre M, Gonczy P. The arithmetic of centrosome biogenesis. J Cell Sci 2004;117:1619–29.
2. Lingle WL, Barrett SL, Negron VC, et al. Centrosome amplification drives chromosomal instability in breast tumor development. Proc Natl Acad Sci U S A 2002;99: 1978–83.
3. Pihan GA, Purohit A, Wallace J, Malhotra R, Liotta L, Doxsey SJ. Centrosome defects can account for cellular and genetic changes that characterize prostate cancer progression. Cancer Res 2001;61:2212–9.
4. Fukasawa K, Choi T, Kuriyama R, Rulong S, Vande Woude GF. Abnormal centrosome amplification in the absence of p53. Science 1996;271:1744–7.
5. Harvey M, Sands AT, Weiss RS, et al. *In vitro* growth characteristics of embryo fibroblasts isolated from p53-deficient mice. Oncogene 1993;8:2457–67.
6. Tutt A, Gabriel A, Bertwistle D, et al. Absence of Brca2 causes genome instability by chromosome breakage and loss associated with centrosome amplification. Curr Biol 1999;9:1107–10.
7. Zhou H, Kuang J, Zhong L, et al. Tumour amplified kinase *STK15/BTAK* induces centrosome amplification, aneuploidy, and transformation. Nat Genet 1998;20: 189–93.
8. Pastink A, Eeken JCJ, Lohman PHM. Genomic integrity and the repair of double-strand DNA breaks. Mutat Res 2001;480-481:37–50.
9. Valerie K, Povirk LF. Regulation and mechanisms of mammalian double-strand break repair. Oncogene 2003; 22:5792–812.
10. West SC. Molecular views of recombination proteins and their control. Nat Rev Mol Cell Biol 2003;4:435–45.
11. Xu X, Weaver Z, Linke SP, et al. Centrosome amplification and a defective G_2-M cell cycle checkpoint induce genetic instability in BRCA1 exon 11 isoform-deficient cells. Mol Cell 1999;3:389–95.
12. Yamaguchi-Iwai Y, Sonoda E, Sasaki MS, et al. Mre11 is essential for the maintenance of chromosomal DNA in vertebrate cells. EMBO J 1999;18:6619–29.
13. Griffin CS, Simpson PJ, Wilson CR, Thacker J. Mammalian recombination-repair genes *XRCC2* and *XRCC3* promote correct chromosome segregation. Nat Cell Biol 2000;2:757–61.
14. Dodson H, Bourke E, Jeffers LJ, et al. Centrosome amplification induced by DNA damage occurs during a prolonged G_2 phase and involves ATM. EMBO J 2004;23: 3863–73.
15. Smiraldo PG, Gruver AM, Osborn JC, Pittman DL. Extensive chromosomal instability in *Rad51d*-deficient mouse cells. Cancer Res 2005;65:2089–96.
16. Hsu L-C, White RL. BRCA1 is associated with the centrosome during mitosis. Proc Natl Acad Sci U S A 1998;95:12983–8.
17. Rice MC, Smith ST, Bullrich F, Havre P, Kmiec EB. Isolation of human and mouse genes based on homology to REC2, a recombinational repair gene from the fungus *Ustilago maydis*. Proc Natl Acad Sci U S A 1997;94:7417–22.
18. Sigurdsson S, Van Komen S, Bussen W, Schild D, Albala JS, Sung P. Mediator function of the human Rad51B-Rad51C complex in Rad51/RPA-catalyzed DNA strand exchange. Genes Dev 2001;15:3308–18.
19. Lio Y-C, Mazin AV, Kowalczykowski SC, Chen DJ. Complex formation by the human Rad51B and Rad51C DNA repair proteins and their activities *in vitro*. J Biol Chem 2003;278:2469–78.
20. Yokoyama H, Kurumizaka H, Ikawa S, Yokoyama S, Shibata T. Holliday junction binding activity of the human Rad51B protein. J Biol Chem 2003;278:2767–72.
21. Liu Y, Masson J-Y, Shah R, O'Regan P, West SC. RAD51C is required for Holliday junction processing in mammalian cells. Science 2004;303:243–6.
22. Takata M, Sasaki MS, Sonoda E, et al. The Rad51 paralog Rad51B promotes homologous recombinational repair. Mol Cell Biol 2000;20:6476–82.
23. Shu Z, Smith S, Wang L, Rice MC, Kmiec EB. Disruption of *muREC2/RAD51L1* in mice results in early embryonic lethality which can be partially rescued in a $p53^{-/-}$ background. Mol Cell Biol 1999;19:8686–93.
24. Thacker J. The *RAD51* gene family, genetic instability, and cancer. Cancer Lett 2005;219:125–35.
25. Schoenmakers EFPM, Huysmans C, Van de Ven WJM. Allelic knockout of novel splice variants of human recombination repair gene *RAD51B* in t(12;14) uterine leiomyomas. Cancer Res 1999;59:19–23.
26. Ingraham SE, Lynch RA, Kathiresan S, Buckler AJ, Menton AG. *hREC2*, a *RAD51*-like gene, is disrupted by t(12;14)(q15;q24.1) in a uterine leiomyoma. Cancer Genet Cytogenet 1999;115:56–61.
27. Takahashi T, Nagai N, Oda H, Ohama K, Kamada N, Miyagawa K. Evidence for *RAD51L1/HMGIC* fusion in the pathogenesis of uterine leiomyoma. Genes Chromosomes Cancer 2001;30:196–201.
28. Quade BJ, Weremowicz S, Neskey DM, et al. Fusion transcripts involving *HMGA2* are not a common molecular mechanism in uterine leiomyomata with rearrangements in 12q15. Cancer Res 2003; 63:1351–8.
29. Amant F, Debiec-Rychter M, Schoenmakers EFPM, Hagemeijer-Hausman A, Vergote I. Cumulative dosage effect of a *RAD51L1/HMGA2* fusion and RAD51L1 loss in a case of pseudo-Meigs' syndrome. Genes Chromosomes Cancer 2001;32:324–9.
30. Blank C, Schoenmakers EFPM, Rogalla P, et al. Intragenic breakpoint within RAD51L1 in a t(6;14)(p21.3;q24) of a pulmonary chondroid hamartoma. Cytogenet Cell Genet 2001;95:17–9.
31. Nicodeme F, Geffroy S, Conti M, et al. Familial occurrence of thymoma and autoimmune diseases with the constitutional translocation t(14;20)(q24.1;p12.3). Genes Chromosomes Cancer 2005;44:154–60.
32. Miyagawa K, Tsuruga T, Kinomura A, et al. A role for *RAD54B* in homologous recombination in human cells. EMBO J 2002;21:175–80.
33. Tashiro S, Walter J, Shinohara A, Kamada N, Cremer T. Rad51 accumulation at sites of DNA damage and in postreplicative chromatin. J Cell Biol 2000;150:283–91.
34. Gough NM. Rapid and quantitative preparation of cytoplasmic RNA from small numbers of cells. Anal Biochem 1988;173:93–5.
35. Sonoda E, Sasaki MS, Morrison C, Yamaguchi-Iwai Y, Takata M, Takeda S. Sister chromatid exchanges are mediated by homologous recombination in vertebrate cells. Mol Cell Biol 1999;19:5166–9.
36. Bishop DK, Ear U, Bhattacharyya A, et al. Xrcc3 is required for assembly of Rad51 complexes *in vivo*. J Biol Chem 1998;273:21482–8.
37. Takata M, Sasaki MS, Tachiiri S, et al. Chromosome instability and defective recombinational repair in knockout mutants of the five Rad51 paralogs. Mol Cell Biol 2001;21:2858–66.
38. Yoshihara T, Ishida M, Kinomura A, et al. XRCC3 deficiency results in a defect in recombination and increased endoreduplication in human cells. EMBO J 2004;23:670–80.
39. Thompson LH, Schild D. Homologous recombinational repair of DNA ensures mammalian chromosome stability. Mutat Res 2001;477:131–53.
40. Deans B, Griffin CS, O'Regan P, Jasin M, Thacker J. Homologous recombination deficiency leads to profound genetic instability in cells derived from *Xrcc2*-knockout mice. Cancer Res 2003;63:8181–7.
41. Deans B, Griffin CS, Maconochie M, Thacker J. *Xrcc2* is required for genetic stability, embryonic neurogenesis, and viability in mice. EMBO J 2000;19:6675–85.
42. Masson J-Y, Tarsounas MC, Stasiak AZ, et al. Identification and purification of two distinct complexes containing the five RAD51 paralogs. Genes Dev 2001;15: 3296–307.
43. Liu N, Schild D, Thelen MP, Thompson LH. Involvement of Rad51C in two distinct protein complexes of Rad51 paralogs in human cells. Nucleic Acids Res 2002;30:1009–15.
44. Daboussi F, Thacker J, Lopez BS. Genetic interactions between RAD51 and its paralogues for centrosome fragmentation and ploidy control, independently of the sensitivity to genetoxic stresses. Oncogene 2005;24: 3691–86.
45. Hut HMJ, Lemstra W, Blaauw EH, van Cappellen GWA, Kampinga HH, Sibon OCM. Centrosome split in the presence of impaired DNA integrity during mitosis. Mol Biol Cell 2003;14:1993–2004.
46. Marx J. Debate surges over the origins of genomic defects in cancer. Science 2002;297:544–6.
47. Quintyne NJ, Reing JE, Hoffelder DR, Gollin SM, Saunders WS. Spindle multipolarity is prevented by centrosomal clustering. Science 2005;307:127–9.
48. Tarapore P, Fukasawa K. Loss of p53 and centrosome hyperamplification. Oncogene 2002;21:6234–40.
49. Sluder G, Nordberg JJ. The good, the bad, and the ugly: the practical consequences of centrosome amplification. Curr Opin Cell Biol 2004;16:49–54.

Published online February 2, 2006

880–892 Nucleic Acids Research, 2006, Vol. 34, No. 3
doi:10.1093/nar/gkj495

Haploinsufficiency of the Mus81–Eme1 endonuclease activates the intra-S-phase and G_2/M checkpoints and promotes rereplication in human cells

Takashi Hiyama[1,3], Mari Katsura[1], Takashi Yoshihara[1], Mari Ishida[1], Aiko Kinomura[1], Tetsuji Tonda[2], Toshimasa Asahara[3] and Kiyoshi Miyagawa[1,4,*]

[1]Department of Human Genetics and [2]Department of Environmetrics and Biometrics, Research Institute for Radiation Biology and Medicine and [3]Department of Surgery, Graduate School of Biomedical Sciences, Hiroshima University, 1-2-3 Kasumi, Minami-ku, Hiroshima 734-8553, Japan and [4]Section of Radiation Biology, Graduate School of Medicine, The University of Tokyo, 7-3-1 Hongo, Bunkyo-ku, Tokyo 113-0033, Japan

Received November 21, 2005; Revised and Accepted January 23, 2006

ABSTRACT

The Mus81–Eme1 complex is a structure-specific endonuclease that preferentially cleaves nicked Holliday junctions, 3′-flap structures and aberrant replication fork structures. *Mus81*$^{-/-}$ mice have been shown to exhibit spontaneous chromosomal aberrations and, in one of two models, a predisposition to cancers. The molecular mechanisms underlying its role in chromosome integrity, however, are largely unknown. To clarify the role of Mus81 in human cells, we deleted the gene in the human colon cancer cell line HCT116 by gene targeting. Here we demonstrate that Mus81 confers resistance to DNA crosslinking agents and slight resistance to other DNA-damaging agents. Mus81 deficiency spontaneously promotes chromosome damage such as breaks and activates the intra-S-phase checkpoint through the ATM-Chk1/Chk2 pathways. Furthermore, Mus81 deficiency activates the G_2/M checkpoint through the ATM-Chk2 pathway and promotes DNA rereplication. Increased rereplication is reversed by the ectopic expression of Cdk1. Haploinsufficiency of Mus81 or Eme1 also causes similar phenotypes. These findings suggest that a complex network of the checkpoint pathways that respond to DNA double-strand breaks may participate in some of the phenotypes associated with Mus81 or Eme1 deficiency.

INTRODUCTION

Precise replication of the entire genome during the S phase of the cell cycle is essential for cell survival. The progression of replication forks can be stalled in response to exogenous and endogenous sources, including depletion of deoxyribonucleotide pools, inhibition of replication proteins and aberrant DNA structures. Stalled replication forks can degenerate into broken forks, leading to chromosomal rearrangements and deletions (1). To avoid such deleterious events, all eukaryotes have evolved cell cycle checkpoint machinery and DNA repair pathways (2). The homologous recombination repair pathway contributes to the accurate repair of DNA damage; however, to promote cell survival, homologous recombination also participates in chromosomal rearrangements when replication forks are stalled (3).

Mus81 was originally identified as a member of the XPF family of endonucleases that physically interacts with Rad54 in *Saccharomyces cerevisiae* and Cds1 (Chk2) in *Schizosaccharomyces pombe* (4,5). The gene confers resistance to agents that lead to replication fork stalling or collapse, including ultraviolet (UV) radiation, methylmethane sulfonate (MMS), hydroxyurea and camptothecin, suggesting a role for Mus81 in the rescue of stalled and collapsed replication forks (6). In contrast, Mus81-deficient murine cells are not hypersensitive to camptothecin (7). The functional binding partner of the protein is MMS4 in *S.cerevisiae* (8) and Eme1 in *S.pombe* (9) and mammals (10–13). The synthetic lethality of *mus81* (or *mms4*) *sgs1* (or *top3*) double mutants suggests a functional link between Mus81 and Sgs1 helicases in the late steps of recombination (4,8). *In vitro*, the Mus81–Eme1 complex preferentially cleaves 3′-flap structures, various aberrant replication fork structures, and nicked Holliday junctions, suggesting that the complex plays a role in stalled replication fork processing and DNA repair by homologous recombination (14–16).

Loss of Mus81, MMS4 or Eme1 results in a reduction in sporulation and spore viability in yeast (8,9,17). Poor spore viability in *mus81* or *eme1* mutants of *S.pombe* is suppressed

*To whom correspondence should be addressed. Tel: +81 358413503; Fax: +81 358413013; Email: miyag-tky@umin.ac.jp

by eliminating Rec6 or Rec12, proteins required for the formation of double-strand breaks (DSBs), which initiates meiotic recombination. Expression of the bacterial Holliday junction resolvase RusA has been found to rescue the *mus81* meiotic defect (9). Thus, Mus81, MMS4 and Eme1 have been implicated in the processing of homologous recombination intermediates in yeast meiosis. The role of the Mus81–Eme1 complex in mitotic homologous recombination in mammals, however, remains uncertain (10,11,18). Remarkably, both *Mus81*$^{+/-}$ and *Mus81*$^{-/-}$ mice exhibit a profound predisposition to lymphomas and other cancers (18), although a subsequent study found no increased susceptibility to cancer in a different *Mus81*$^{-/-}$ model (7).

The role of Mus81 in genome integrity in response to replication stress has been proposed to be related to its physical association with Cds1 (Chk2) in fission yeast (19). Cds1-dependent phosphorylation of Mus81 prevents it from cleaving stalled replication forks that lead to replication fork breakage and chromosomal rearrangements by dissociating it from chromatin in cells exposed to hydroxyurea. Spontaneous and mitomycin C (MMC)-induced DNA damage such as breaks and triradial exchanges is increased in *Mus81*$^{+/-}$ and *Mus81*$^{-/-}$ mouse cells. In addition to these aberrations, the mutant cells have been shown to have an increased rate of aneuploidy (18).

Despite accumulating evidence that Mus81 plays a role in the processing of aberrant replication fork structures, the molecular mechanisms underlying its role in chromosome stability remain unclear. To clarify the role of Mus81–Eme1 in human cells, we deleted the genes in the human colon cancer cell line HCT116 by gene targeting. The advantages of using this cell line are that it allows efficient gene targeting in the presence of an intact p53 gene (20) and the cellular ploidy is stable. Here we show that Mus81 deficiency activates the intra-S-phase and G_2/M checkpoints and promotes DNA rereplication. This promotion of DNA rereplication was reversed by the forced expression of Cdk1. These findings provide new insight into the role of the Mus81–Eme1 complex in the control of human cell ploidy.

MATERIALS AND METHODS

Gene targeting at the Mus81 and Eme1 loci in HCT116

Targeting vectors were designed for in-frame insertion of promoterless drug resistance genes in exon 3 of *Mus81* or in exon 2 of *Eme1*. A 2.5 kb 5′-homology arm of *Mus81* was amplified by PCR from the isogenic DNA of HCT116 cells using primers 5′-GCCATGTCCAACGTCAGTA-3′ and 5′-ATCGATTCTCTCCAGATGGTGAGT-3′. A 1.7 kb 3′-homology arm of *Mus81* was amplified using primers 5′-ATCGATACTTGCGGAAGTCCA-3′ and 5′-AGGCAGAGGGGACAACACAG-3′. A 2.6 kb 5′-homology arm of *Eme1* was amplified using primers 5′-TTCACAGCACTTGCCAGTCT-3′ and 5′-ATCGATAATCCAGTGAGGGTGATGAC-3′. A 1.8 kb 3′-homology arm of *Eme1* was amplified using primers 5′-ATCGATTGTGAAGCCTCCTGTCCT-3′ and 5′-GGAACTGTCCTGTGTTACTG-3′. Both arms were cloned into pCR2.1 (Invitrogen) by the TA cloning method. The 3′-arms of *Mus81* and *Eme1* were excised by digestion with ClaI/SpeI and ClaI/XhoI, respectively, and subcloned into the vectors containing the 5′-arms. Neomycin and blasticidin resistance cassettes were inserted into the ClaI site of the vector containing both arms. Gene targeting in HCT116 was performed as described previously (21).

Ectopic expression of the Mus81 and Eme1 cDNAs

The human *Mus81* cDNA was amplified by PCR from cDNA derived from normal human cells using primers 5′-TGATCTCAACGGTCCTGC-3′ and 5′-GGGCTGTTTCACGGCATAA-3′. The human *Eme1* cDNA was amplified using primers 5′-AGTTGAAAGAGTGGCGGGA-3′ and 5′-CTCATCCCTGAGGGCTAGAA-3′. The cDNAs were inserted into pCR2.1, and the sequences were confirmed. The expression vectors were designed to insert the genes under the control of the MSV enhancer and the MMTV promoter. Transfected cells were selected in the presence of 900 μg/ml Zeocin™ (Invitrogen).

Sensitivity to DNA-damaging agents

Sensitivity to MMC was measured as described previously (22). To measure sensitivity to hydroxyurea, we plated the cells at a density of 2×10^3 cells per 60 mm dish, treated them with the agent for 6 h, and washed them three times with phosphate-buffered saline (PBS). To measure the sensitivity to UV treatment, we plated the cells at the same density and irradiated them. After 7 days of culturing, colonies were counted. Sensitivity to other DNA-damaging agents was measured as described previously (21). When knockout or complemented cells showed slow growth compared to wild-type cells, colonies were further cultured for 2 to 3 days and counted.

Focus formation of Rad51 and Rad54

Radiation-induced focus formation of Rad51 and Rad54 was performed as described previously (21). MMC-induced focus formation was examined by treatment with 0.8 μg/ml MMC for 1 h.

Cell cycle analysis

Cell synchronization by double-thymidine block was performed as described previously (23). Flow cytometry was performed with a FACSCalibur (Becton Dickinson) using the CellQuest software package.

Kinase assay

Immunoprecipitation was performed in the presence of phosphatase inhibitors (5 μM cantharidin, 5 nM microcystin LR and 25 μM bromotetramisole oxalate) essentially as described (22). Immunoprecipitates were washed three times in lysis buffer and three times in 25 mM HEPES (pH 7.4). The kinase reaction was performed at 30°C for 20 min in a total of 40 μl of reaction buffer [25 mM HEPES (pH 7.4), 15 mM $MgCl_2$, 80 mM EGTA, 1 mM DTT, 0.1 mM ATP and 3 μCi [γ-^{32}P]ATP]. Histone H1 (10 μg) was used as a substrate for the cyclin E, cyclin A and cyclin B kinase assays. Glutathione *S*-transferase (GST)-Cdc25C (200–256) was used as a substrate for the Chk2 kinase assay and was prepared as follows. The Cdc25C (200–256) fragment was amplified by PCR from cDNA derived from normal human cells using primers 5′-GAAAGATCAAGAAGCAAAGGTGAGC-3′ and 5′-TAAGCCCTTCCTGAGCTT-3′ and inserted into pGEX-5X-1